Massive and permanent decline of symbiont bearing morozovellids and $\delta^{13}C$ perturbations across the Early Eocene Climatic Optimum at the Possagno section (Southern Alps of northeastern Italy)

V**aleria Luciani [1] , Jan Backman [2], Eliana Fornaciari[3], Luca Giusberti [3], Claudia Agnini [3], Roberta D'Onofrio**[1]

[1]Department of Physics and Earth Sciences, Ferrara University, Polo Scientifico Tecnologico, via G. Saragat 1, 44100, Ferrara, Italy

[2]Department of Geological Sciences, Stockholm University, SE-10691 Stockholm, Sweden

[3]Department of Geosciences, Padova University, via G. Gradenigo 6, 35131, Padova, Italy

Correspondence to: V. Luciani (valeria.luciani@unife.it)

Abstract - The Early Eocene Climatic Optimum (EECO) records the highest prolonged global temperatures over the past 90 Ma. Understanding the causes and timing of Eocene climate change remains a major challenge in Cenozoic paleoceanography, which includes the biotic response to climate variability and the changes among planktic foraminiferal assemblages across the EECO. The symbiont bearing and shallow dwelling genera *Morozovella* and *Acarinina* were important calcifiers in the tropical-subtropical early Paleogene oceans but almost completely disappeared at about 38 Ma, near the Bartonian/Priabonian boundary. We show here that morozovellids record a first critical step across the EECO through a major permanent decline in relative abundance from the Tethyan Possagno section and ODP Site 1051 in the western subtropical North Atlantic. Possible causes may include increased eutrophication, weak water column stratification, changes in ocean chemistry, loss of photosymbionts and possible complex interaction with other microfossil groups. Relative abundances of planktic foraminiferal taxa at Possagno parallel negative shifts in both $\delta^{13}C$ and $\delta^{18}O$ of bulk sediment from Chron C24r to basal Chron C20r. The post-EECO stable isotopic excursions towards lighter values are of modest intensity. Significant though ephemeral modifications in the planktic foraminiferal communities occur during these minor isotopic

excursions. These modifications are marked by pronounced increases in relative abundance of acarininids, in a manner similar to their behaviour during pre-EECO hyperthermals in the Tethyan settings, which suggest a pronounced biotic sensitivity to climate change of planktic foraminifera even during the post-EECO interval.

1 Introduction

The Early Eocene Climatic Optimum (EECO) is the interval in which the Earth's climate attained its warmest state of the past 90 Ma and it represents a major turning point in the Cenozoic climate, as it was followed by a long term cooling throughout the remainder of the Eocene, which culminated with the formation of permanent large ice sheets on Antarctica at the end of the Eocene (Zachos et al., 2001; Coxall et al., 2005). Superimposed on the long term early Eocene climate trend, short lived (<200 kyr) warm events occurred, named hyperthermals, the most extreme of which is the well known Paleocene Eocene Thermal Maximum (PETM) (Agnini et al., 2009; Coccioni et al., 2012; Cramer et al., 2003; Kennett and Stott, 1991; Lourens et al., 2005; Nicolò et al., 2007; Quillévéré et al., 2008; Zachos et al., 2008). Massive, rapid releases of isotopically light carbon are linked to hyperthermals and concomitant deep-sea carbonate dissolution events (Dickens, 2011; Dickens et al., 1995, 1997; Zachos et al., 2005, 2008). The series of early Eocene hyperthermals (Littler et al., 2014; Slotnick et al., 2012; Zachos et al., 2010) has been suggested to continue into the earliest middle Eocene, with an additional thirteen brief (~40 kyr) and less pronounced events (Kirtland Turner et al., 2014; Sexton et al., 2011).

Although the EECO still lacks a formal definition in terms of absolute age and duration (Slotnick et al., 2012), this interval is thought to represent a ca. 2-3 Ma long early Eocene interval of extreme warmth between about 52 and 50 Ma (Zachos et al., 2001) or between about 53 Ma and 51 Ma (Zachos et al., 2008). Current thought about the placement of the EECO thus encompasses the interval from approximately 50 Ma to 53 Ma. Regardless of the exact duration and position on the chronometric scale of the EECO, it is clearly much longer than any of the brief early Eocene hyperthermals (Zachos et al., 2001; 2008; 2010). Exceptionally high and long lasting atmospheric pCO_2 conditions are considered to have played a primary control on the EECO warmth (Fletcher et al., 2008; Hyland and Sheldon, 2013; Komar et al., 2013; Lowenstein and Demicco, 2006; Pearson and Palmer, 2000; Smith et al., 2010). Slow addition of depleted carbon dioxide from volcanism, the second emplacement phase

of the North Atlantic Igneous Province, and increased weathering of silicate rocks are often invoked as the main trigger of the EECO warming and the subsequent long term cooling trend (Demicco, 2004; Raymo and Ruddiman, 1992; Sinton and Duncan, 1998; Vogt, 1979; Zachos et al., 2008). The influence of a major switch from continental to island arc volcanism around 50 Ma may also have played a role in perturbing the carbon cycle change that helped end the warm EECO interval (Dickens et al., 2014; Lee et al., 2013).

It is well established that major plant and mammal faunal evolutionary turnovers occurred during the EECO (Falkowski et al., 2005; Figueirido et al., 2012; Wilf et al., 2003; Wing et al., 1991; Woodbourne et al., 2009; Zonneveld et al., 2000). In the marine realm, changes in evolutionary trends have also been observed, for example the inception to the modern structure among calcareous nannofossil communities (Agnini et al., 2006; Shamrock and Watkins, 2012; Schneider et al., 2011) and possibly in diatom lineages (Oreshkina, 2012; Sims et al., 2006). These observations both from continents and the oceans support the hypothesis of a primary interaction between climate change and biotic evolution.

The relationship between the EECO and the paleoecology and evolution of planktic foraminifera is insufficiently known. At the beginning of the Eocene, planktic foraminiferal history was far enough from the Cretaceous-Paleogene mass extinction to have originated several phylogenetic lines with taxa occupying different ecological niches in the upper water column. The Eocene is a crucial interval in evolution of planktic foraminifera that encompassed one of their major diversifications reaching a peak in the middle Eocene (Norris, 1991; Pearson et al., 2006).

Within this plankton group, the symbiont bearing and shallow dwelling morozovellids and acarininids are of particular interest because they dominated the tropical and subtropical assemblages of the early Paleogene oceans. These genera belong to the muricate group, from the muricae that form conical pustules on the test wall. Among calcareous microplankton, the muricates were one of the major calcifiers in the low latitude early Paleogene oceans and almost completely disappeared at about 38 Ma, near the Bartonian/Priabonian boundary (Agnini et al., 2011; Luciani et al., 2010; Wade, 2004; Wade et al., 2012).

The hemipelagic Possagno sedimentary succession is located in the Venetian Prealps of northeastern Italy (Fig. 1). This section represents continuous deposition of the early through early middle Eocene interval (55-46 Ma) from a bathyal setting in the central-western Tethys. A robust

Eocene biomagnetostratigraphy was established by Agnini et al. (2006). The Possagno section thus spans the EECO interval, here agreed as the interval from about 53 to 50 Ma (Slotnick et al., 2012).

According to Agnini et al. (2006), the Possagno section is 66 m thick extending from the Paleocene/Eocene boundary at about 56 Ma to the early middle Eocene (lower Chron C20r) at 46 Ma on the time scale of Cande and Kent (1995). The aim here is to investigate the response of the muricates in terms of relative abundance throughout the early and early middle Eocene, including the EECO interval, in the 56 Ma through 46 Ma interval at Possagno, encompassing biozones planktic foraminiferal Zones E1 to lower E8 (Luciani and Giusberti, 2014). In addition, the planktic foraminiferal changes recorded at Possagno are compared with those observed from ODP Site 1051 in the western subtropical North Atlantic. Additional aims include (1) to document planktic foraminiferal changes in the Possagno section in relation to stable carbon and oxygen isotopes for the purpose to unravel paleoenviromental conditions of the upper water column and (2), to distinguish ephemeral biotic modifications during brief peaks of warming from permanent evolutionary changes in the Tethyan and North Atlantic realms.

2 The Possagno section and Site 1051: setting and stratigraphy

An upper Cretaceous-Miocene succession crops out at the bottom of the Monte Grappa Massif in the Possagno area, about 60 km NW of Venice. The lower to middle Eocene interval, which is the focus of this study, is represented by pelagic to hemipelagic Scaglia facies sediments. The Scaglia beds at Possagno are considered to have been deposited at middle to lower bathyal depths (Cita, 1975; Thomas, 1998) in the western part of the Belluno Basin, a Mesozoic–Cenozoic paleogeographic unit of the Southern Alps characterized by Jurassic to Eocene pelagic sequences (Bosellini, 1989). The basal part of the Possagno section straddles a 30 cm thick interval of dark-red clayey marls (Arenillas et al., 1999; Agnini et al., 2006), referred to as the Clay Marl Unit (CMU) by Giusberti et al. (2007). The CMU is the lithological expression of the main carbon isotope excursion (CIE) of the Paleocene Eocene Thermal Maximum (PETM), the base of which defines the Paleocene-Eocene boundary (Aubry et al., 2007). The bio- lithostratigraphic assignment of the Possagno sediments follows Luciani and Giusberti (2014), and the magnetostratigraphy is from Agnini et al. (2006) (Figs. 2,3).

The Blake Nose is a gentle ramp extending from 1000 m to 2700 m water depth at the Blake

Escarpment in the western North Atlantic (Norris et al, 1998). ODP Site 1051 is located well above the local lysocline and the carbonate compensation depth. The sediments studied here are from 452.24 to 353.10 meters below sea floor (mbsf) and consists of lower to middle Eocene carbonate ooze and chalk (Norris et al., 1998). This part of the Eocene section shows good recovery except between 382 mbsf and 390 mbsf (Fig. 4) and contains abundant calcareous plankton. Magnetostratigraphy is from Ogg and Bardot (2001). Paleodepth estimates from benthic foraminiferal assemblages indicate lower bathyal depth (1000-2000 m) during late Paleocene-middle Eocene (Norris et al., 1998). Bohaty et al. (2009) derived a paleodepth of about 2200 m for the interval around to 50 Ma through a standard subsidence model.

3 Methods

Analyses of foraminifera and stable isotopes were performed from the identical sample set of the Possagno section previously used for calcareous nannofossils (Agnini et al., 2006). Relative abundances have been determined from about 300 specimens extracted from each of the 110 samples investigated in the >63 µm size fraction. A sampling interval of 2–5 cm was used in the basal 0.7 m of the Possagno section, followed by 50 cm spacing for the 0.7–14 m interval, and 20 cm for the 14-66 m interval. Washed residues were prepared following standard procedures, which varied with the different lithologies. Foraminifera were successfully extracted from the indurated marly limestones and limestones using the cold-acetolyse technique (Lirer, 2000; Luciani and Giusberti, 2014), a highly successful method for disaggregating strongly lithified samples (Fornaciari et al., 2007; Luciani et al., 2007), otherwise analyzable only in thin section. The marly samples were disaggregated using 30 % hydrogen peroxide and subsequently washed and sieved using a 63 µm sieve. In most cases, gentle ultrasonic treatment improved the cleaning of the tests. In the Possagno section, foraminifera are continuously present and diverse throughout the studied interval with a preservation varying from moderate to fairly good, even though tests are recrystallized and essentially totally filled.

The weight percent of the >63 µm size fraction relative to the weight of the bulk sample, typically 100 g/sample, for the 110 Possagno samples is referred to as the coarse fraction, following Hancock and Dickens (2005). Investigation of fifty Eocene samples at Site 1051 (Hole 1051A) from 452.24 to

353.1 mbsf, corresponding to ~52-47 Ma, had a spacing varying from 2.0 m to 0.5 m. These were prepared using disaggregation using distilled water and washing over 38 μm and 63 μm sieves. Washed residues were dried at <50°C. Planktic foraminifera from Site 1051 are abundant and well preserved.

The degree of dissolution, expressed as fragmentation index (*F* index), has been evaluated by counting the number of planktic foraminiferal fragments or partially dissolved tests versus entire tests on 300 elements, following Hancock and Dickens (2005). These data are expressed in percentages. Fragmented foraminifera include specimens showing missing chambers and substantial breakage.

Carbon and oxygen stable isotope data of bulk sediment samples were analysed using a Finnigan MAT 252 mass spectrometer equipped with a Kiel device at Stockholm University. Precision is within ±0.06 ‰ for carbon isotopes and ±0.07 ‰ for oxygen isotopes. Stable isotopes values are calibrated to the Vienna Pee Dee Belemnite standard (VPDB) and converted to conventional delta notation ($\delta^{13}C$ and $\delta^{18}O$).

4 Results

4.1 Foraminiferal fragmentation

The *F* index recorded at Possagno (Fig. 3) displays a large variability throughout the interval investigated. The highest values, up to 70 %, were observed in the 16-22 m interval. The maximum *F* index values correspond to the minimum values in the $\delta^{13}C$ record. A number of *F* index peaks mimic the $\delta^{13}C$ negative peaks below 16 m, showing values between 60 % and 70 %.

F index values at Site 1051 (Fig. 4) show less variability with respect to Possagno. A maximum value of 60 % is reached in Zone E5, just below an interval of uncertain magnetostratigraphic attribution (Norris et al., 1998), here referred to as Chron C23r. Relatively high *F* index values around 50 % occur the upper portions of Chrons C24n and C22r. The interval across the EECO, on the basis of biomagnetostratigraphic correlation and here placed between ca 397 and 425 mbsf, displays *F* index values (<20 %). The relatively lower *F* index values at Site 1051 are presumably caused by less carbonate dissolution at that site and, to some extent, the lower resolution of the investigated samples at Site 1051.

4.2 Weight percent coarse fraction

Carbonate dissolution generally causes the bulk sediment coarse fraction to decrease because of fragmentation of foraminiferal tests (Hancock and Dickens, 2005). The coarse fraction and *F* index data from Possagno (Fig. 3) do not show such an anti-phasing, especially in the post-EECO interval. The coarse fraction at Possagno shows minor fluctuations with a mean value of 5.3±1.5 % from the base of the EECO and upsection, with pre-EECO values varying around 10 %.

4.3 Carbon and oxygen isotopes

The $\delta^{13}C$ data from Possagno show a negative shift of about 1.5 ‰ at the 0 m level, which corresponds to the Paleocene-Eocene boundary (Agnini et al., 2009) There are nine additional negative carbon isotope excursions above the Paleocene-Eocene boundary in the lower 21.4 m of the Possagno section (Fig. 2, Tab. S1):

1. 0.9 ‰ at 21.4 m (C22r) within EECO
2. 1.1 ‰ at 20.8 m (C22r) within EECO
3. 0.6 ‰ at 19.8 m (C23n) within EECO
4. 0.8 ‰ at 18.0 m (C23n) within EECO
5. 0.9 ‰ at 16.8 m (C23n) within EECO
6. 0.4 ‰ at 14.8 m (C24n.1n) within EECO (X event)
7. 0.3 ‰ at 12.5 m (near C24n.2n/C24n.2r boundary; J event)
8. 0.3 ‰ at 10.5 m (mid C24n.3n; I event)
9. 0.3 ‰ at 8.0 m (upper C24r; ETM2/ELMO event)

The two oldest of these carbon isotope excursions are determined using 45-50 cm sample spacing, implying that their true magnitudes are probably not fully captured. Their precise positions may also change as higher resolution data become available from this relatively condensed part of the section showing sedimentation rates <0.5 cm/kyr. The remaining five are determined using 20 cm sample spacing. The number, magnitudes and stratigraphy of the above carbon isotope excursions are similar to the results of other studies (Agnini et al., 2009; Slotnick et al., 2012; Zachos et al., 2010).

Above Chron C22r, a series of additional minor negative carbon isotope excursions (CIEs) are recorded in Chron C22n, Chron C21r and Chron C21n from the Possagno section. By combining the chron identification with the number of CIEs starting at the old end of the chron, these CIEs are coined C22n-CIE1, C22n-CIE2, etc., up to C21n-CIE4 (Fig. 2). We have tentatively named the isotope shifts of small magnitude as events only when changes in isotopic composition are associated with evident modifications in planktic foraminferal assemblages and/or in fragmentation index. This is because increase in both fragmentation index and some foraminiferal taxa is similar to the record observed during early Eocene hyperthermals from the same geological setting (Luciani et al. 2007; Agnini et al., 2009). As the Possagno section is measured from the base of the PETM (0 m) and upsection, increasing distance from the PETM level yields increasing positive meter values:

1. C21n-CIE4 − 0.3 ‰ from 56.6 m to 57.0 m
2. C21n-CIE3 − 0.3 ‰ from 55.6 m to 56.2 m
3. C21n-CIE2 − 0.3 ‰ from 54.8 m to 55.0 m
4. C21n-CIE1 − 0.8 ‰ from 48.8 m to 49.4 m
5. C21r-CIE4 − 0.3 ‰ from 39.6 m to 39.8 m
6. C21r-CIE3 − 0.5 ‰ from 38.8 m to 39.2 m
7. C21r-CIE2 − 0.7 ‰ from 37.6 m to 38.2 m
8. C21r-CIE1 − 0.9 ‰ from 32.8 m to 33.2 m
9. C22n-CIE3 − 0.5 ‰ from 31.2 m to 31.4 m
10. C22n-CIE2 − 0.5 ‰ from 30.0 to 30.2 m
11. C22n-CIE1 − 0.6 ‰ from 27.2 m to 27.4 m

Oxygen isotopes of bulk rock measurements from indurate marly limestones and limestones may be affected by diagenetic overprints (Marshall, 1992), which presumably apply also to the rocks in the Possagno section. Despite of this preservation caveat, it is assumed that oscillations in oxygen isotopes chiefly represent temperature fluctuations during the ice-free early Eocene world. Lighter oxygen isotope values in the Possagno section indeed show a clear correspondence with lighter carbon isotope values (CIEs) and vice versa in the post-EECO interval (Fig. 2). Thus, despite the possibility of some diagenetic overprinting in several individual samples, especially in the lower part of our record, a three-point moving average of oxygen isotope data should reveal early to early middle Eocene climate variability in the Possagno section.

241

242 **4.4 Planktic foraminiferal quantitative analysis**

243

244 The planktic foraminiferal assemblages show significant modifications in the early to early
245 middle Eocene interval at Possagno (Fig. 3). The mean relative abundance of *Acarinina* is about 46 %
246 of the total assemblage throughout the section. Members of this genus show peak abundances of 60-70
247 % of the total assemblage during the early to early middle Eocene CIEs. Particularly prominent is the
248 increase to ~80 % during the EECO interval (Fig. 3). Acarininids clearly thrived and expanded in
249 abundance during the CIEs, including the EECO.

250 This increase of acarininids is counter balanced by a transient decrease in members of
251 subbotinids. This latter group recovers above the EECO interval and increases moderately from ~24 %
252 to ~36 % in terms of mean relative abundance of the total assemblage, up to the top of the section. The
253 North Atlantic Site 1051 also shows a slight increase of ca. 7 % in the mean value among the
254 subbotinids during the corresponding time interval.

255 A permanent reduction in the abundance of members of the genus *Morozovella* represents a
256 major change within the planktic foraminiferal assemblages within Zone E5. This group collapses from
257 a mean value of ~24 % in the 0-15 m interval to less than 6 % above 15 m. Qualitative examination of
258 species variability shows that, in the lower part of the Zone E5 where the greater morozovellids
259 abundance is recorded, no dominance of particular species is recognized, even though *M.*
260 *marginodentata*, *M. subbotinae* and *M. lensiformis* are relatively more common forms with respect to
261 *M. aequa*, *M. aragonensis*, *M. formosa* and *M. crater*. In the interval with the low abundance of
262 morozovellids within the EECO, an overturn is observed since *M. aragonensis*, *M. formosa*, *M. crater*
263 and, in the upper part of the E5 Zone, *M. caucasica* are the most common species.

264 Morozovellids never recover to their pre-EECO abundances, even if including the appearance of
265 the ecologically comparable genus *Morozovelloides* (Pearson et al., 2006) in samples above 36 m.

266 Genera and species with low abundances show minor changes throughout the interval studied at
267 Possagno (Fig. S1).

268 The major change in planktic foraminiferal assemblages at Site 1051 includes a distinct decrease of
269 *Morozovella*, from mean values around 40 % to 10 % in the middle part of Zone E5 (Fig. 4). Similarly
270 to Possagno, the lower part of Zone E5 with the higher percentages of morozovellids does not record

the dominance of selected species, but at Site 1051 *M. aragonensis* and *M. formosa* besides *M. subbotinae* are relatively common whereas *M. marginodentata* is less frequent. Within the interval of low morozovellid abundances, *M. aragonensis* and *M. formosa* are the most common taxa. The general decline of morozovellids does not appear therefore related, both at Possagno and Site 1051, to the extinction or local disappearance of a dominant species.

The differences in the relative abundance of morozovellids at Possagno and Site 1051 indicate a morozovellid preference for open ocean settings of low-latitudes, as suggested also by other authors (Berggren, 1978; Boersma et al., 1987; Premoli Silva and Boersma, 1988). Like at Possagno, morozovellids never recover at Site 1051 in the Zone E5 through E8 interval. The abundance of subbotinids shows little variations around mean values of 20 % at Site 1051. *Acarinina* displays an increase in mean relative abundance from 35 % (base to ca. 450 mbsf) to around 50 % (ca. 430 mbsf), with maximum values of about 60 %. The relatively low resolution used here does not permit comparison between the early Eocene CIEs at Site 1051 (Cramer et al., 2003) and how the relative abundance of planktic foraminiferal genera varies with respect to CIEs.

4.5 Radiolarian abundance

Radiolarians are rare to absent in the Possagno section. Brief temporary occurrences of this group have been observed in coincidence with some of the most negative $\delta^{13}C$ excursions. Specifically, they reach a maximum relative abundance of 28 % in the lower part of the major $\delta^{13}C$ perturbation recorded in the lower to middle part of C23n, of ~10 % at 27.5 m and of 15 % at 31.4 m (Fig. 3). At Site 1051, radiolarians fluctuate in abundance from 0 to 78 % throughout the studied interval.

5. Discussion

5.1 The $\delta^{18}O$ and $\delta^{13}C$ stratigraphies at Possagno

The $\delta^{18}O$ and $\delta^{13}C$ records from the Possagno section display both details and trends (Fig. 2) that are similar to those observed in several other late Paleocene through early middle Eocene stable isotope

301 stratigraphies (Cramer et al., 2009; Schmitz et al., 1997; Shackleton et al., 1985; Slotnick et al., 2012;
302 Zachos et al., 2001; 2008). For example, the major CIE (-1.5 ‰) close to the base of the Possagno
303 section represents the PETM, followed upsection by hyperthermals ETM2, I, J, and ETM3 (Agnini et
304 al., 2009). The initiation and termination of the EECO are not well constrained in any single
305 sedimentary record (Slotnick et al., 2012), nor so at Possagno, yet the interval between 16 m and 22.5
306 m in Possagno shows the lightest $\delta^{18}O$ values during the entire post-PETM interval of the early Eocene
307 and early middle Eocene (Fig. 2) and is considered to represent at least part of the EECO. In terms of
308 oxygen isotope stratigraphy, both the EECO and post-EECO intervals are characterized by a series of
309 rapid oscillations. The oxygen isotope amplitude range shows up to 1.5 ‰ differences between
310 adjacent samples, which possibly may reflect potential diagenetic overprint. By running a 3-point
311 running mean of the oxygen isotope data, single overprint outliers are dampened. Even so, these data
312 show rapid amplitude changes of up to 0.5 ‰, suggesting correspondingly rapid temperature changes
313 in the western Tethys on the order of 2°C during the ice-free early and early middle Eocene world. The
314 underlying cause of these distinct and rapid temperature changes may be sought in the stable carbon
315 isotope data.
316 Several lines of evidence suggest that high CO_2 concentrations were driving the EECO global
317 warmth as well as the hyperthermal events of the early Eocene (Fletcher et al., 2008; Hyland and
318 Sheldon, 2013; Komar et al., 2013; Lowenstein and Demicco, 2006; Lunt et al., 2011; Pearson and
319 Palmer, 2000; Royer et al., 2007; Smith et al., 2010). A series of CIEs occur within and above the
320 EECO interval at Possagno. A number of CIEs have been observed from ODP Site 1258 in the western
321 tropical Atlantic (Kirtland Turner et al., 2014; Sexton et al., 2006; 2011), which they interpreted as
322 minor hyperthermals and referred to as 21 numbered H-events (H for Hyperthermal) in Chrons C23r
323 through C21r. Sedimentation rates at Possagno are 2-6 times lower than those at Site 1258 in the
324 indentical time interval. The number of CIEs within individual magntochron zones at Possagno and
325 Site 1258 differ slightly, presumably because of differences in sedimentation rates and sample
326 resolution. Kirtland Turner et al. (2014) listed three CIEs/H-events in Chron C23r, none of which are
327 evident in the Possagno record at the present sample resolution, probably due to strongly condensed
328 sedimentation or presence of a hiatus. At Possagno, three events are recorded in C23n, compared with
329 the two CIEs/H-events from Demerara Rise, whereas only two of the six CIEs/H-events in Chron C22r
330 are distinguishable in Possagno. Five CIEs/H-events are listed in Chron C22n from Demerara Rise,

three of which are evident in the Possagno record. Finally, five CIEs/H-events are listed in Chron C21r, four of which are evident in the Possagno record. It follows that the lower sample resolution at Possagno likely has blurred both the number and true magnitudes of the isotopic amplitude changes. It remains uncertain if the CIEs and H-events at Site 1258 and the CIEs in the Possagno section are in synchrony (Tab. 1).

Regardless of the potential synchrony between Possagno and Site 1258 at the Demerara Rise, both regions clearly demonstrate that after the EECO, from ca. 50 Ma to ca. 46-47 Ma during a trend of cooling (2-2.4°C) climate, about 18 brief negative CIEs coincide with hyperthermal-like brief episodes of warming. These brief CIEs induced environmental perturbations that are expressed in the planktic foraminiferal data from the Possagno section. This points to a primary relationship between increased CO_2 concentration and warmth during early through early middle Eocene times (Dickens et al., 2005; Quillévéré et al., 2008; Zachos et al., 2005; 2008;).

5.2 The EECO interval and hyperthermals at Possagno: Acarinina dominated or dissolution controlled assemblages?

One of the most prominent changes in the planktic foraminiferal assemblages is the dominance of acarininids across the EECO interval, resulting in a corresponding decrease in relative abundance of morozovellids and subbotinids (Fig. 3). These changes parallel relatively high values of the *F* index and coincide with the most negative parts in the $\delta^{13}C$ record. The increase in shell fragmentation suggests some carbonate dissolution. The high pCO_2 atmospheric concentration during the EECO may have induced carbonate dissolution at the deep-water Possagno setting, resulting from deep-water acidification and a rise of the lysocline, similar to patterns observed during the main hyperthermal events. This interpretation for the Possagno section should however imply a considerable shallowing of the CCD/lysocline, assuming that the section was deposited in a middle to lower bathyal setting. Further studies on the Tethyan CCD in the Eocene interval will help investigate the hypothesis that the CCD was shallower there, with respect to the open ocean CCD. Intensified water column remineralization of organic matter, forced by augmented metabolic rates at elevated temperatures, may have caused pH to decrease in the uppermost water column, inducing dissolution of calcitic tests (Brown et al., 2004; John et al., 2013, 2014; O'Connor et al., 2009; Olivarez Lyle and Lyle, 2006).

Questions arise on how to estimate the possible dissolution artefacts from the primary ecological signal. Nguyen et al. (2011) and Petrizzo et al. (2008) studied Pacific Ocean assemblages of latest Paleocene to initial Eocene age, and suggested that subbotinids are more dissolution susceptible than morozovellids and acarininds, which previously were thought to be the most dissolution prone forms (Berggren and Norris, 1997; Boersma and Premoli Silva, 1983). Paleogene assemblages affected by extensive dissolution could be expected to be impoverished with respect to the more dissolution susceptible subbotinids. These results have been challenged by other analyses that document a dominance of subbotinids within intervals affected by a high *F* index and enhanced carbonate dissolution (Luciani et al., 2010), who suggested that dissolution has affected the planktic assemblages rather equally. The degreee of dissolution of planktic foraminifera appears to have varied during different time intervals, being species related rather than exclusively associated with different genera. However, since data on dissolution susceptibility on different genera are so far lacking for early and early middle Eocene times, we cannot exclude that dissolution may have changed the planktic foraminiferal assemblages.

When assuming that dissolution has affected assemblages, it follows that the dominance of acarininids during the EECO and hypertermal events may represent a taphonomic artifact. This assumption appears yet to conflict with the results from the upper part of Possagno in the Chron C21n interval, where significant decreases of subbotinids, associated with distinct acarininid increases, correspond to negative shifts in $\delta^{13}C$ values in the absence of carbonate dissolution, as expressed in low *F* index values (Fig. 3).

The similarity in the major planktic foraminiferal modifications throughout the EECO at Site 1051(Fig. 4), which appears only marginally affected by dissolution, suggests that the Possagno assemblages represent a reasonably genuine paleoecological response rather than assemblages primarily modified by carbonate dissolution.

The decrease of CF values (Fig. 3) in the EECO interval might indicate loss of carbonate shells due to carbonate dissolution. Similarly, relatively low CF-values with only minor fluctuations are recorded to the top of the section, independently from changes in *F* index values. The CF curve parallels the EECO/post-EECO trend of the morozovellid abundance thus suggesting a relationship with the morozovellid decline rather than carbonate dissolution.

5.3 The Possagno and Site 1051 records: planktic foraminiferal response to the EECO

The planktic foraminiferal assemblages show significant variations in the Possagno material that correlate with the pronounced $\delta^{13}C$ perturbations in the EECO interval (Fig. 3). When the warm preferring acarininds become dominant during the EECO, this results in a reduction in relative abundance of the warm preferring morozovellids. This feature is recurring in planktic foraminiferal assemblages across some hyperthermals (PETM and X events), as recorded from a number of Tethyan successions of northeastern Italy and it has been interpreted as a result of relatively enhanced eutrophication of surface waters in a near continental setting (Agnini et al., 2009; Arenillas et al., 1999; Luciani et al., 2007; Molina et al., 1999).

Planktic foraminiferal analyses of the pre-EECO hyperthermals ETM2, I, J and ETM3 at Possagno show PETM-like responses, consisting of strongly increasing relative abundances of acarininids, as in the PETM interval of the nearby Forada section (Luciani et al., 2007). The multi-proxy analyses of the X-event at the nearby Farra section (Agnini et al., 2009) corroborate at higher resolution the record from Possagno. Increased surface water eutrophication has been proposed to favour acarininids, in being able to temporarily colonize deeper waters that previously were occupied by subbotinids and in being able to tolerate relatively high eutrophic conditions that suppressed the abundances of morozovellids (Agnini et al., 2009; Luciani et al., 2007). Slight differences in paleobiology between morozovellids and acarininids are documented in several cases by minor variations in stable isotopes that commonly indicate a more surface habitat for the former group (Boersma et al., 1987; Pearson et al., 1993; 2001).

The increased surface water eutrophication during hyperthermals was forced by strengthening of the hydrological cycle and increased weathering as a consequence to enhanced greenhouse conditions. The effects improved the nutrient availability in this near continental, pelagic setting of the western Tethys (Agnini et al., 2009: Giusberti et al., 2007; Luciani et al., 2007). The hypothesis of increased nutrient availability in the lower part of the EECO interval at Possagno is supported by the entry of relatively high concentration of radiolarians, considered as eutrophic indices (Hallock, 1987).

The decline of morozovellids across the EECO at Possagno and Site 1051 is irreversible and cannot be explained by brief perturbations, as during the pre-EECO hyperthermals. The morozovellid crisis is coupled with the gradual disappearances of several species, including *M. aequa*, *M. gracilis*,

M. lensiformis, *M. marginodentata*, and *M. subbotinae*, and it is not counterbalanced by the appearance of species of *Morozovelloides*, a minor component of middle Eocene assemblages. The latter genus appeared at Possagno around the Ypresian/Lutetian boundary (Luciani and Giusberti, 2014) and it is morphologically highly convergent with *Morozovella* although probably did evolve from *Acarinina* (Pearson et al., 2006).

The similar behaviour across the EECO of morozovellids in the Tethyan Possagno section and Site 1051 in the western subtropical North Atlantic supports the hypothesis of a geographically wide spread morozovellid crisis that is caused by climate change. This change must be a consequence of the major modifications across the EECO, both in terms of temperature and pCO_2, which in turn must have induced water column reorganizations leading to a reduction of the morozovellid habitat. Because morozovellids exhibit transient reduction in abundance during pre-EECO hyperthermals, and due to the imprecise definition of this event, it is not possible to precisely pinpoint the exact turning point of the morozovellid decline, i.e. whether it began just at the onset, within, or at the termination of the EECO event. Current data from Possagno and Site 1051 however record that their massive drop in abundance began across the C24n1n-C23r transition. The decrease apparently started at the top of C24n1n at Possagno, but it has not been possible to determine whether or not this decrease is transitory because a potential recovery may be hidden by condensation/hiatus across the C24n1n-C23r interval. Present data from Site 1051 record the decline in lower C23r, even though some uncertainties are caused by the low resolution in the foraminiferal analysis and magnetostratigraphic attribution.

In contrast to the deterioration of the morozovellid habitat, relatively favourable conditions for thermocline dwellers such as subbotinids and parasubbotinids are suggested by the new species appearing progressively during the post-EECO interval at Possagno (Luciani and Giusberti, 2014), in good agreement with the low latitude data presented by Pearson et al. (2006). Most of the new species will characterize the thermocline of the middle and late Eocene oceans: *Subbotina corpulenta*, *S. eocena*, *S. hagni*, *S. senni*, *S. yeguanesis*, *Parasubbotina griffinae*, and *P. pseudowilsoni*. The appearance of the radially chambered *Parasubbotina eoclava*, which is considered to be the precursor of the truly clavate chambered *Clavigerinella* (Coxall et al., 2003; Pearson and Coxall, 2014) occurs at 19.8 m (Luciani and Giusberti, 2014). *Clavigerinella* is the ancestor of the genus *Hantkenina* that successfully inhabited the sub-surface middle through late Eocene oceans. Prior to the evolution of genuine *Clavigerinella*, *P. eoclava* made several aborted attempts to evolve towards the genus

Clavigerinella. This is reflected in presence of rare and scattered specimens that are morphologically close to *Clavigerinella* within the EECO interval even though true representative of genus *Clavigerinella* were not observed in the Possagno section.

The EECO and post-EECO intervals indeed proved to be crucial in Eocene planktic foraminferal evolution.

5.4 Possible causes of morozovellids decline across the EECO

The data from Possagno and Site 1051 demonstrate that the early Paleogene planktic foraminiferal symbiont bearing groups were strongly affected by a habitat deterioration across the EECO. The early Eocene crisis was followed by a second step, involving the large sized acarininids and *Morozovelloides*, documented through their reduction in abundance as well as test size during the Middle Eocene Climate Optimum (MECO) at ca. 40 Ma in Tethyan (Fig. 5), Southern Ocean, and northwest Atlantic settings (Edgar et al., 2012; Luciani et al., 2010). Furthermore, the muricate crisis culminates near the Bartonian/Priabonian boundary with a major demise in the *Acarinina* lineage and the extinction of *Morozovelloides*. Only small (<125 μm) and relatively rare acarininids survived into the late Eocene and Oligocene (Agnini et al., 2011; Berggren et al., 2006; Wade, 2004; Wade et al., 2012). An episode with loss of symbiosis resulting in bleaching caused by global warming has been proposed to explain the second muricate crisis (Edgar et al., 2012). If the MECO warmth has been the main cause of bleaching of acarininids, we would expect that this phenomenon also involved morozovellids during the EECO, as this warm interval records the highest temperatures of the Paleogene. Considering the importance of photosymbiosis in extant species for foraminiferal test calcification and ecology (Bé, 1982; Bé et al., 1982; Hemleben et al., 1989), we may assume similar requirements for fossil taxa. The algal-symbiotic relationship is considered one of the most successful strategies adopted by muricates during the earliest Paleogene (Norris, 1996; Quillévéré et al., 2001). A crisis in that relationship may represent one possible hypothesis to explain the decline of early Eocene morozovellids. Further studies that include stable isotope analyses, including $\delta^{13}C$ gradients, on morozovellid tests are needed to further elucidate this scenario. There is however scarce documentation on mechanisms responsible for bleaching and besides elevated sea surface temperature, a number of other factors, for example high ultraviolet radiation, decrease in pH decrease, increase in CO_2, changes

481 in salinity and nutrient availability, may have been involved (Douglas et al., 2003; Wade et al., 2008)).

482 The protracted exceptional warming of the EECO is expected to have increased metabolic rates
483 particularly in heterotrophs that are more sensitive to temperature than rates of primary production
484 (Brown et al., 2004; O'Connor et al., 2009; Olivarez Lyle and Lyle, 2006). This effect may have
485 increased water column remineralization of organic matter and caused pH to decrease in the uppermost
486 water column (John et al., 2013; 2014; O'Connor et al., 2009; Olivarez Lyle and Lyle, 2006). The
487 potential lowering of pH in surface waters, which could have been further enhanced by the huge EECO
488 CO_2 pressure, may have affected calcification (De Moel et al., 2009; Moy et al., 2009; Zeebe et al.,
489 2008) of most surface dwellers such as the morozovellids, also by reducing or completely halting their
490 symbiont relationships.

491 Complex interactions with other microfossil groups, such as radiolarians, diatoms or
492 dinoflagellates, may have contributed to the morozovellid crisis across the EECO, for example by
493 competing for the use of the same algal-symbionts in the case of radiolarians, or symbiont-providers.
494 Detailed comparisons of trends in other fossil groups are necessary to investigate this hypothesis.

495 Seawater chemistry influences the biomineralization of organisms producing $CaCO_3$ skeletons,
496 especially for many algae and invertebrates that have less control over the chemical composition of
497 their mineralized parts (Stanley, 2006; 2008). High magnesium/calcium ratios are known to have
498 favoured aragonitic and high-Mg calcite skeletons throughout the Phanerozoic. This insight is
499 corroborated by experiments with living organisms, confirming, for example, population growth
500 among the calcitic coccolithophores in conditions of low concentration of Mg and high concentration
501 of calcium in seawater (Stanley et al., 2005). A strong reduction in Ca concentration occurred during
502 the Cenozoic, following the 'calcitic' Cretaceous ocean, possibly driven by changes in rates of deep-
503 sea igneous activity (Hardie, 1996). We cannot exclude that a decrease of Ca concentration in seawater
504 chemistry may have affected morozovellid calcification. Planktonic foraminifera have not been widely
505 employed to study the effects of the Mg/Ca ratio of the seawater on calcification, however, they have
506 been found to produce heavier skeleton when the saturation state of the ambient seawater with respect
507 to calcite is elevated. It would be interesting to compare flux data of calcareous nannofossils before and
508 after the major evolutionary change recorded across the EECO (Agnini et al., 2006; Schneider et al.,
509 2011) to test a potential reduction in their overall productivity.

510 Extended time intervals of weak water column stratification and increased eutrophication are

known to provide hostile ecological conditions for the highly specialized oligotrophic morozovellids (Boersma et al., 1987; Bralower et al., 1995; Pearson et al., 2006; Premoli Silva and Boersma, 1989). Such conditions are documented in several ocean sites by the recorded decline in surface-to-benthic $\delta^{13}C$ gradients (Hilting et al., 2008) and have been considered linked to evolutionary turnovers among calcareous nannofossil assemblages (Schneider et al., 2011). Weakened thermal stratification with increased vertical mixing is predicted for many, although not all, oceanic areas during hyperthermals. The fact that the permanent morozovellid collapse occurs during the EECO implies that a threshold was surpassed, not previously experienced by the morozovellid communities.

Available data indicate that the protracted conditions of extreme warmth and high CO_2 pressure during the EECO may have been the key element inducing a permanent impact in the marine surface water ecosystem that became detrimental for the morozovellids. Even the peculiar PETM, that records the most dramatic changes among the hyperthermals both in terms of temperature increase and carbon cycle perturbation, did not adversely affected the morozovellid habitat in a permanent way. On the contrary, morozovellids increased in abundance in open oceanic settings (Kelly et al., 1996; 1998, 2002; Lu and Keller, 1993; Petrizzo, 2007), and only a transient decrease in abundance is recorded in pelagic Tethyan near continental settings (Luciani et al., 2007). It is intriguing to note that the second main crisis of the muricate symbiont bearing forms occurred during the MECO (Fig. 5), that is also a warming event of much longer duration (about 400-500 kyr) than the early Paleogene hyperthermals (Bohaty et al., 2009; Westerhold and Röhl, 2013).

5.5 Planktic foraminiferal changes during post-EECO stable-isotope perturbations at Possagno

The small $\delta^{13}C$ excursions recorded in the post-EECO interval at Possagno, from C22n to C21n, induced perturbations on the planktic foraminiferal assemblages that mirror those recorded in the pre-EECO interval (Fig. 3). These perturbations are expressed as marked increases of acarininids, representing warmer thriving taxa that were tolerant to relatively enhanced surface water eutrophic conditions. Peaks in surface water eutrophication could have been reached during the C22n-CIE1 and C22n-CIE3 events, as indicated by the relatively high production of radiolarians.

The post-EECO CIEs are concomitant with $\delta^{18}O$ excursions and coupled to distinct modifications in the planktic foraminiferal assemblages comparable to those recorded at other early Eocene brief

warming events in Tethyan settings. These data make it tenable to refer to these events as hyperthermals, although of less intensity and magnitude compared to some of the pre-EECO hyperthermals. A number of these $\delta^{13}C$ and $\delta^{18}O$ excursions, of much smaller magnitude and intensity with respect to the PETM, probably correlate with the recently discovered late early Eocene through early middle Eocene post-EECO hyperthermals in the Atlantic and Pacific (Kirtland Turner et al., 2014; Sexton et al., 2006; 2011; Tab.1). According to Sexton et al. (2011) and Kirtland Turner et al. (2014) their shorter duration and more rapid recovery phases, with respect to the PETM, imply a different forcing and feedback mechanism involving redistribution of carbon among the ocean reservoirs rather than release of greenhouse gases from buried sediments. This mechanism was active also during the EECO interval and was similar to the orbital forcing of the carbon cycle operating during the Oligocene and Miocene.

6 Summary and conclusions

The investigation of planktic foraminifera from the Possagno section in northern Italy represents a first case history recording changes in relative abundance among planktic foraminiferal assemblages across the EECO warm interval and post-EECO climatic variability in the Tethys realm from about 55 Ma to 46 Ma.

The most crucial change emerging from the Possagno and ODP Site 1051 data is the irreversible decline across the EECO of the symbiont bearing genus *Morozovella*, one of the most important calcifiers of the early Paleogene tropical and subtropical oceans. The Possagno data indicate that the EECO event had a permanent impact on the planktic foraminiferal communities, representing a critical phase in the reorganization of Eocene pelagic ecosystems. Possible causes for this reorganization, that deserve further investigations, include increased eutrophication, changes in ocean chemistry, weak water column stratification, loss of symbionts, complex interaction with other microplankton groups such us radiolarians, diatoms or dinoflagellates that represented possible competitors in the use of symbionts or as symbiont providers. A critical threshold was reached across the EECO, evidently never reached before, which induced unfavourable habitats for continued morozovellid diversification and proliferation but not harsh enough to cause their extinction. This threshold appears to be related to the

duration of extreme conditions characterizing the extended warmth during the EECO.

Even though several questions still remain to be answered, the data presented from Possagno add significant information about the complex evolution of the muricate planktic foraminifera and stimulate additional investigations across the EECO from different paleoceanographic settings.

The post-EECO interval at Possagno is punctuated by relatively small, negative $\delta^{13}C$ shifts, interpreted as potential minor hyperhthermals in the light of available oxygen isotope data, a number of which probably are in synchrony with those recorded in the tropical Atlantic by Sexton et al. (2011) and Kirtland Turner et al. (2014). These modest post-EECO $\delta^{13}C$ and $\delta^{18}O$ perturbations are associated with significant, though ephemeral, modifications in the planktic foraminiferal communities showing distinct increases of the warm acarininids in a manner similar to their behaviour during pre-EECO hyperthermals in Tethyan settings. Changes in planktic foraminiferal assemblages occur during environmental perturbations associated with minor negative carbon and oxygen isotope excursions, which suggest a pronounced biotic sensitivity to climate change of planktic foraminifera even during the post-EECO interval.

Acknowledgements. Funding for this research was provided by MIUR/PRIN COFIN 2010-2011, coordinated by D. Rio. V. Luciani was financially supported by FAR from Ferrara University, and L. Giusberti and E. Fornaciari received financial support from Padova University (Progetto di Ateneo GIUSPRAT10 CPDA108242/10). J. Backman acknowledges support from the Swedish Research Council. We are grateful to Domenico Rio who promoted the researches on the "Paleogene Veneto" and for the fruitful discussion. Members of the "Possagno net", Simone Galeotti, Dennis Kent, Giovanni Muttoni, who sampled the section in 2003, are gratefully acknowledged**.** We warmly acknowledge the Cementi Rossi s.p.a. and Mr. Silvano Da Roit for fruitful collaboration during samplings at the Carcoselle Quarry (Possagno, TV). This research used samples and data provided by the Ocean Drilling Program (ODP). ODP is sponsored by the U.S. National Science Foundation (NSF) and participating countries under management of Joint Oceanographic Institution (JOI) Inc. We specially thank from the ODP Bremen Core Repository. Finally, we are grateful to the reviewers, B.Wade and R. Speijer, who helped to strengthen the manuscript.

References

Agnini, C., Muttoni, G., Kent, D.V., Rio, D.: Eocene biostratigraphy and magnetic stratigraphy from Possagno, Italy: the calcareous nannofossils response to climate variability, Earth Planet. Sci. Lett., 241, 815–830, 2006.

Agnini, C., Macrì, P., Backman, J., Brinkhuis, H., Fornaciari, E., Giusberti, L., Luciani, V., Rio, D., Sluijs, A., Speranza, F.: An early Eocene carbon cycle perturbation at □52.5 Ma in the Southern Alps: chronology and biotic response, Paleoceanogr., 24, PA2209. doi:10.1029/2008PA001649, 2009

Agnini, C., Fornaciari, E., Giusberti, L., Grandesso, P., Lanci, L., Luciani, V., Muttoni, G., Plike, H., Rio, D., Spofforth, D. J. A., Stefani, C.: Integrated biomagnetostratigraphy of the Alano section (NE Italy): a proposal for defining the middle-late Eocene boundary, Geol. Soc. Am. Bull., 123, 841–872, 2011.

Arenillas, I., Molina, E., Schmitz, B.: Planktic foraminiferal and $\delta^{13}C$ isotopic changes across the Paleocene/Eocene boundary at Possagno (Italy), Int. J. Earth Sc., 88, 352–364, 1999.

Aubry, M.-P., Ouda, K., Dupuis, C., Berggren, W.A., Van Couvering, J.A., and the Members of the Working Group on the Paleocene-Eocene Boundary.: The Global Standard Stratotype-Section and Point (GSSP) for the base of the Eocene Series in the Dababiya section (Egypt)., Episodes 30, 271–286, 2007.

Be´, A.W.H.: Biology of planktonic foraminifera, in: Foraminifera: notes for a short course, Broadhead T., Stud. Geol., 6, Univ. Knoxville, Tenn., 51–92, 1982.

Be´, A.W.H., Spero, H.J., Anderson O.R.: Effects of symbiont elimination and reinfection on the life processes of the planktonic foraminifer *Globigerinoides sacculifer*, Marine Biol. 70, 73–86, 1982.

Berggren, W.A.: Rates of evolution in some Cenozoic planktonic foraminifera, Micropaleont. 15, 337-

370, 1978.

Berggren, W.A., Norris, R.D.: Biostratigraphy, phylogeny and systematics of Paleocene trochospiral planktic foraminifera, Micropaleont., 43 (Suppl. 1), 1–116, 1997.

Berggren, W. A., Pearson, P. N., Huber, B.T., Wade, B. S.: Taxonomy, Biostratigraphy and Phylogeny of Eocene Acarinina, In: Atlas of Eocene Planktonic Foraminifera, Cushman Foundation Spec. Publ. 41, Pearson, P. N., Olsson, R. K., Huber, B.T., Hemleben, C., Berggren, W. A., 257–326, 2006.

Boersma, A., Premoli Silva, I.: Paleocene planktonic foraminiferal biogeography and the paleoceanography of the Atlantic-Ocean, Micropaleont., 29, 4, 355–381, 1983.

Boersma, A., Premoli Silva, I., Shackleton, N.: Atlantic Eocene planktonic foraminiferal biogeography and stable isotopic paleoceanography, Paleoceanogr., 2, 287–331, 1987.

Bohaty, S.M., Zachos, J.C., Florindo, F., Delaney, M.L.: Coupled greenhouse warming and deep-sea acidification in the Middle Eocene, Paleoceanogr., 24, PA2207, doi:10.1029/2008PA001676, 2009.

Bosellini, A.: Dynamics of Tethyan carbonate platform, in: Controls on Carbonate Platform and Basin Platform, Crevello, P.D., Wilson, J.L., Sarg, J.F., Read, J.F., SEPM Spec. Publ., 44, 3–13, 1989.

Bralower, T.J., Zachos, J.C., Thomas, E., Parrow, M., Paull, C.K., Kelly, D.C., Premoli Silva, I., Sliter, W.V., Lohmann, K.C.: Late Paleocene to Eocene paleoceanography of the equatorial Pacific Ocean: Stable isotopes recorded at Ocean Drilling Program Site 865, Allison Guyot, Paleoceanogr., 10, 841–865, 1995.

Brown, J.H., Gillooly, J.F., Allen, A.P., Savage, V.M., and West, G.B.: Toward a metabolic theory of ecology, Ecology, 85(7), 1771–1789, 2004.

Cande, S. C., Kent, D. V.: Revised calibration of the geomagnetic polarity timescale for the Late

661 Cretaceous and Cenozoic, J. Geophys. Res., 100, 6093–6095, 1995.
662
663 Cita, M. B.: Stratigrafia della Sezione di Possano. In Bolli, H. M. (Ed.), Monografia
664 Micropaleontologica sul Paleocene e l'Eocene di Possagno, Provincia di Treviso, Italia, Schweiz.
665 Palaeontol. Abhandl., 97, pp.9–33, 1975.
666
667 Coccioni, R., Bancalà, G., Catanzariti, R., Fornaciari, E., Frontalini, F., Giusberti, L., Jovane, L.,
668 Luciani, V., Savian, J., Sprovieri, M.: An integrated stratigraphic record of the Palaeocene–lower
669 Eocene at Gubbio (Italy): new insights into the early Palaeogene hyperthermals and carbon isotope
670 excursions, Terra Nova, 24, 380–386, 2012.
671
672 Coxall, H. K., Wilson, P.A; Pälike, H.; Lear, C. H; Backman, J.: Rapid stepwise onset of Antarctic
673 glaciation and deeper calcite compensation in the Pacific Ocean. Nature, 433, 53-57,
674 doi:10.1038/nature03135, 2005.
675
676 Cramer, B.S., Wright, J.D., Kent, D.V., Aubry, M.-P.: Orbital climate forcing of $\delta^{13}C$ excursions in the
677 late Paleocene–early Eocene (chrons C24n–C25n), Paleoceanogr., 18, 21-1.
678 doi:10.1029/2003PA000909, 2003.
679
680 Cramer, B.S., Toggweiler, J.R., Wright, M.E., Katz, J.D., Miller, K.G.: Ocean overturning since the
681 Late Cretaceous: Inferences from a new benthic foraminiferal isotope compilation, Paleoceanogr., 24,
682 PA4216, doi:10.1029/2008PA001683, 2009.
683
684 Coxall, H.K., Huber, B.T., Pearson, P.N.: Origin ad morphology of the Eocene planktic foraminifera
685 *Hantkenina*, J. Foram. Res., 33, 237-261, 2003.
686
687 Coxall, H. K., Wilson, P.A; Pälike, H.; Lear, C. H; Backman, J.: Rapid stepwise onset of Antarctic
688 glaciation and deeper calcite compensation in the Pacific Ocean. Nature, 433, 53-57,
689 doi:10.1038/nature03135, 2005.
690

De Moel, H., Ganssen G.M., Peeters F.J.C., Jung, S.J.A., Kroon, D., Brummer, G.J.A., Zeebe, R.E.: Planktic foraminiferal shell thinning in the Arabian Sea due to anthropogenic ocean acidification? Biogeosciences, 6, 1917-1925, 2009.

Demicco, R.V.: Modeling seafloor-spreading rates through time, Geology 32, 485- 488, 2004.

Dickens, G.R.: Methane release from gas hydrate systems during the Paleocene–Eocene Thermal Maximum and other past hyperthermal events: setting appropriate parameters for discussion, Clim. Past., 7(2), 1139–1174. doi:10.5194/cpd-7-1139-2011, 2011.

Dickens, G.R., O'Neil, J.R., Rea, D.K., Owen, R.M.: Dissociation of oceanic methane hydrate as a cause of the carbon isotope excursion at the end of the Paleocene, Paleoceanogr., 10, 965–971, doi:10.1029/95PA02087, 1995.

Dickens, G.R., Castillo, M.M., Walker, J.C.G.: A blast of gas in the latest Paleocene: simulating first-order effects of massive dissociation of oceanic methane hydrate, Geology, 25, 259–262, 1997.

Dickens G.R., Lee C.A., CIA Operatives: Continental - island arc fluctuations through time and the Eocene transition from a greenhouse to an icehouse world, Rend. Online Soc. Geol. It., 31, 62-63. doi: 10.3301/ROL.2014.46, 2014.

Douglas, A.E.: Coral bleaching- how and why? Mar. Pollut. Bull., 46, 385–392, 2003.

Edgar, K.M., Bohaty, S.M., Gibbs, S.J., Sexton, P.F., Norris, R.D., Wilson, P.A.: Symbiont 'bleaching' in planktic foraminifera during the Middle Eocene Climatic Optimum, Geology, 41, 15-18, doi:10.1130/G33388.1, 2012.

Falkowski, P.G., Katz, M.E., Milligan, A.J., Fennel, K., Cramer, B.S., Aubry, M.P., Berner, R.A., Novacek, M.J., Zapol, W.M.: Evolution: The rise of oxygen over the past 205 million years and the evolution of large placental mammals, Science, 309 (5744), 2202-2204, 2005.

721

722 Figueirido, B., Janis, C.M., Pérez-Claros, J.A., De Renzi, M., Palmqvist, P.: Cenozoic climate change
723 influences mammalian evolutionary dynamics, Proc. Natl. Acad. Sci. USA, 109(3), 722-727, 2012.

724

725 Fletcher, B.J., Brentnall, S.J., Anderson, C.W., Berner, R.A., Beerling, D.J.: Atmospheric carbon
726 dioxide linked with Mesozoic and early Cenozoic climate change, Nat. Geosci., 1, 43–48, 2008.

727

728 Fornaciari, E., Giusberti, L., Luciani, V., Tateo, F., Agnini, C., Backman, J., Oddone, M., Rio, D.: An
729 expanded Cretaceous–Tertiary transition in a pelagic setting of the Southern Alps (central–western
730 Tethys), Palaeogeogr. Palaeoclimatol. Palaeoecol., 255, 98–131, 2007.

731

732 Giusberti, L., Rio, D., Agnini, C., Backman, J., Fornaciari, E., Tateo, E., Oddone, M.: Mode and tempo
733 of the Paleocene–Eocene thermal maximum in an expanded section from the Venetian pre-Alps, Geol.
734 Soc. Am. Bull., 119, 391–412, 2007.

735

736 Hallock, P.: Fluctuations in the trophic resource continuum: a factor in global diversity cycles?
737 Paleoceanogr., 2, 457–471, 1987.

738

739 Hancock, H.J.L., Dickens, G.R.: Carbonate dissolution episodes in Paleocene and Eocene sediment,
740 Shatsky Rise, west-central Pacific, in: Bralower, T.J., Premoli Silva, I., Malone, M.J., Proc. ODP, Sci.
741 Results 198. http://www-odp.tamu.edu/publications/198_SR/116/116.htm, 2005.

742

743 Hemleben, C, Spindler, M., Anderson, O.R.: Modern planktonic foraminifera, in: Springer-Verlag,
744 New York, 1-363, ISBN-13: 9780387968155, 1989.

745

746 Hilting, A.K., Kump, L.R., Bralower, T.J.: Variations in the oceanic vertical carbon isotope gradient
747 and their implications for the Paleocene–Eocene biological pump, Paleoceanogr., 23 (3) (PA3222).
748 DOI: 10.1029/2007PA001458, 2008.

749

750 Hyland, E.G., Sheldon, N.D.: Coupled CO2-climate response during the Early Eocene Climatic

751 Optimum, Palaeogeogr. Palaeoclimatol. Palaeoecol., 369, 125-135, 2013.
752
753 John E.H., Pearson P.N., Coxall H.K., Birch H., Wade B.S., Foster G.L.: Warm ocean processes and
754 carbon cycling in the Eocene, Phil. Trans. R. Soc., A, 371, 20130099, 2013.
755
756 John E.H., Wilson J.D., Pearson P.N. Ridgwell A.: Temperature-dependent remineralization and
757 carbon cycling in the warm Eocene oceans, Palaeogeogr. Palaeoclimatol. Palaeoecol., 413, 158-166,
758 2014
759
760 Kelly, D.C., Bralower, T.J., Zachos, J.C., Premoli Silva, I., Thomas, E.: Rapid diversification of
761 planktonic foraminifera in the tropical Pacific (ODP Site 865) during the late Paleocene thermal
762 maximum, Geology 24, 423–426, 1996.
763
764 Kelly, D.C., Bralower, T.J., Zachos, J.C.: Evolutionary consequences of the latest Paleocene thermal
765 maximum for tropical planktonic foraminifera, Palaeogeogr., Palaeoclimatol., Palaeoecol., 141, 139–
766 161, 1998.
767
768 Kennett, J.P., Stott, L.D.: Abrupt deep-sea warming, palaeoceanographic changes and benthic
769 extinctions at the end of the Palaeocene, Nature 353, 225–229, 1991.
770
771 Kirtland Turner S., Sexton P.F., Charled C.D., Norris R.D.: Persistence of carbon release events
772 through the peak of early Eocene global warmth, Nat. Geosc., 7, 748-751, DOI: 10.1038/NGEO2240,
773 2014.
774
775 Komar, N., Zeebe, R.E., Dickens, G.R.: Understanding long-term carbon cycle trends: the Late
776 Paleocene through the Early Eocene, Paleoceanog., 28, 650-662, doi: 10.1002/palo.20060, 2013.
777
778 Lee C.T., Shen B., Slotnick B.S., Liao K., Dickens G.R., Yokoyama Y., Lenardic A., Dasgupta R.,
779 Jellinek M., Lackey J.S., Schneider T., Tice M.M.: Continental arc-island arc fluctuations, growth of
780 crustal carbonates, and long-term climate change, Geosphere, 9, 21-36, 2013.

781

782 Lirer, F.: A new technique for retrieving calcareous microfossils from lithified lime deposits.
783 Micropaleontol., 46, 365–369, 2000.

784

785 Littler, K., Röhl, U., Westerhold, T., Zachos, J.C.: A high-resolution benthic stable-isotope for the
786 South Atlantic: implications for orbital-scale changes in Late Paleocene-early Eocene climate and
787 carbon cycling, Earth Planet. Sci. Lett., 401, 18-30. http://dx.doi.org/10.1016/j.epsl.2014.05.054, 2014.

788

789 Lourens, L.J., Sluijs, A., Kroon, D., Zachos, J.C., Thomas, E., Röhl, U., Bowles, J., Raffi, I.:
790 Astronomical pacing of late Palaeocene to early Eocene global warming events, Nature, 7045, 1083-
791 1087, 2005.

792

793 Lowestein, T.K. Demicco R.V.: Elevated Eocene Atmospheric CO_2 and Its Subsequent Decline,
794 Science, 313 (5795), 1928. DOI:10.1126/science.1129555, 2006.

795

796 Lu, G., Keller, G.: The Paleocene–Eocene transition in the Antarctic Indian Ocean: inference from
797 planktic foraminifera, Mar. Micropaleontol., 21, 101–142, 1993.

798

799 Luciani, V., Giusberti, L., Agnini, C., Backman, J., Fornaciari, E., Rio., D.: The Paleocene–Eocene
800 Thermal Maximum as recorded by Tethyan planktonic foraminifera in the Forada section (northern
801 Italy), Mar. Micropaleont., 64, 189–214, 2007.

802

803 Luciani, V, Giusberti L., Agnini C, Fornaciari E, Rio D, Spofforth D.J.A., Pälike H..: Ecological and
804 evolutionary response of Tethyan planktonic foraminifera to the middle Eocene climatic optimum
805 (MECO) from the Alano section (NE Italy), Palaeogeogr. Palaeoclimatol. Palaeoecol., 292, 82-95, doi:
806 10.1016/j.palaeo.2010.03.029, 2010.

807

808 Luciani, V., Giusberti L.: Reassessment of the early–middle Eocene planktic foraminiferal
809 biomagnetochronology: new evidence from the Tethyan Possagno section (NE Italy) and Western
810 North Atlantic Ocean ODP Site 1051., J. Foram. Res., 44, 2, 187-201, 2014.

Lunt, D.J., Ridgwell, A., Sluijs, A., Zachos, J., Hunter, S., Haywood A.: A model for orbital pacing of methane hydrate destabilization during the Palaeogene, Nat. Geosc. Lett., 4, 775-778, DOI: 10.1038/NGEO1266, 2011.

Marshall, J.D.: Climatic and oceanographic isotopic signals from the carbonate rock records and their preservation, Geol. Mag., 129, 143-160, 1992.

Molina, E., Arenillas, I., Pardo, A.: High resolution planktic foraminiferal biostratigraphy and correlation across the Palaeocene Palaeocene/Eocene boundary in the Tethys, Bull. Soc. Géol. France, 170, 521–530, 1999.

Moy, A.D., Howard, W.R., Bray, S.G., Trull, T.W.: Reduced calcification in modern Southern Ocean planktonic foraminifera, Nat. Geosc., 2, 276-280.doi:10.1038/NGEO460, 2009.

Müller-Merz, E., Oberhänsli, H.: Eocene bathyal and abyssal benthic foraminifera from a South Atlantic transect at 20-30° S, Palaeogeogr. Palaeoclimatol. Palaeoecol., 83, 117-171, 1991.

Nguyen, T.M.P., Petrizzo, M.R., Stassen, P., Speijer, R.P.: Dissolution susceptibility of Paleocene–Eocene planktic foraminifera: Implications for palaeoceanographic reconstructions, Mar. Micropaleont., 81, 1-21, 2011.

Nicolò, M. J., Dickens, G. R., Hollis, C. J., Zachos, J. C.: Multiple early Eocene hyperthermals: their sedimentary expression on the New Zealand continental margin and in the deep sea, Geology, 35, 699–702, 2007.

Norris, R.D.: Biased extinction and evolutionary trends, Paleobiology, 17 (4), 388– 399, 1991.

Norris, R.: Symbiosis as an evolutionary innovation in the radiation of Paleocene planktic foraminifera, Paleobiology, 22, 461–480, 1996.

Norris, R. D., Kroon, D., Klaus, A.: Proceedings of the Ocean Drilling Program, Initial Reports, 171B, Ocean Drilling Program, College Station, TX, p. 1–749, 1998.

O'Connor, M., Piehler, M.F., Leech, D.M., Anton, A., Bruno, J.F.: Warming and resource availability shift food web structure and metabolism, Plos Biol., 7(8), 1-6. doi: 10.1371/journal.pbio.1000178, 2009.

Ogg, J. G., Bardot, L.: Aptian through Eocene magnetostratigraphic correlation of the Blake Nose Transect (Leg 171B), Florida continental margin, in: Proc. Ocean Drill. Progr., Scientific Results, 171B: Ocean Drilling Program, College Station, TX, Kroon, D. et al., 1–58, www.odp.tamu.edu/publications/171B-SR/VOLUME/CHAPTERS/SR171B09, 2001.

Olivarez Lyle, A., and Lyle, M.W.: Missing organic carbon in Eocene marine sediments: Is metabolism the biological feedback that maintains end-member climates? Paleoceanogr., 21, PA2007, doi:10.1029/2005PA001230, 2006.

Oreshkina, T.V.: Evidence of Late Paleocene - Early Eocene hyperthermal events in biosiliceous sediments of Western Siberia and adjacent areas, Austrian J. Earth Sci., 105, 145-153, 2012.

Pearson, P.N., Palmer, M.R.: Atmospheric carbon dioxide concentrations over the past 60 million years, Nature, 406, 695-699, doi:10.1038/35021000, 2000.

Pearson P.N., Coxall H.K.: Origin of the Eocene planktonic foraminifer Hantkenina by gradual evolution, Palaeontology, 57, 243-267, 2014.

Pearson, P.N., Shackleton, N.J., Hall, M.A.: Stable isotope paleoecology of middle Eocene planttonic foraminifera and multi-species isotope stratigraphy, DSDP Site 523, south Atlantic, J. Foram. Res. 23, 123-140, 1993.

Pearson, P.N., Ditchfield, P.W, Singano, J., Harcourt-Brown, K.G., Nicholas, C.J., Olsson, R.K, Shackleton, N.J., Hall, M.A.: Warm tropical sea surface temperatures in the Late Cretaceous and Eocene epochs, Nature 413, 481-487, 2001. doi:10.1038/35097000

Pearson, P.N., Olsson, R.K., Huber, B.T., Hemleben, C., Berggren, W.A.: Atlas of Eocene planktonic foraminifera, in: Cushman Found. Spec. Publ. 1, 1-514, 2006.

Petrizzo, M.R.: The onset of the Paleocene–Eocene Thermal Maximum (PETM) at Sites 1209 and 1210 (Shatsky Rise, Pacific Ocean) as recorded by planktonic foraminifera, Mar. Micropaleont., 63, 187–200, 2007.

Petrizzo, M.R., Leoni, G., Speijer, R.P., De Bernardi, B., Felletti, F.: Dissolution susceptibility of some Paleogene planktonic foraminifera from ODP Site 1209 (Shatsky Rise, Pacific Ocean), J. Foram. Res. 38, 357–371, 2008.

Premoli Silva, I., Boersma, A.: Atlantic Eocene planktonic foraminiferal historical biogeography and paleohygrographic indices, Palaeogeogr. Palaeoclimatol. Palaeoecol. 67, 315-356, 1988.

Premoli Silva, I., Boersma, A.: Atlantic Paleogene planktonic foraminiferal bioprovincial indices, Mar. Micropaleont., 14, 357–371, 1989.

Quillévéré, F., Norris, R.D., Moussa, I., Berggren,W.A.: Role of photosymbiosis and biogeography in the diversification of early Paleogene acarininids (planktonic foraminifera), Paleobiology, 27, 311–326, 2001.

Quillévéré, F., Norris, R.D., Kroon, D., Wilson, P.A.: Transient ocean warming and shift in carbon reservoir during the early Danian, Earth Planet. Sci. Lett., 265, 600–615, 2008.

Raymo, M.E., Ruddiman W.F.: Tectonic forcing of late Cenozoic climate, Nature, 359, 117–122, 1992.

Schmitz, B., Pujalte, V.: Abrupt increase in seasonal extreme precipitation at the Paleocene-Eocene boundary, Geology, 35(3), 215–218, doi:10.1130/G23261A.1, 2007.

Schneider, L.J. Bralower, T.J., Kump, L.J.: Response of nannoplankton to early Eocene ocean destratification, Palaeogeogr. Palaeoclimatol. Palaeoecol., 310, 152-162, 2011.

Sexton, P.F., Wilson, P.A., Norris, R.D.: Testing the Cenozoic multisite composite □□□O and □□□285 C curves: New monospecific Eocene records from a single locality, Demerara Rise (Ocean Drilling Program Leg 207), Paleoceanogr., 21, PA2019, 2006.

Sexton, P.F., Norris R.D., Wilson, P.A., Pälike, H., Westerhold, T., Röhl, U., Bolton, C.T., Gibbs, S.: Eocene global warming events driven by ventilation of oceanic dissolved organic carbon, Nature 471, 349-353, doi:10.1038/nature09826, 2011.

Shackleton, N.J., Corfield, R.M., Hall, M.A.: Stable isotope data and the ontogeny of Paleocene planktonic foraminifera, J. Foraminifer. Res., 15, 321–376, 1985.

Shamrock, J.L., Watkins, D.K., Johnston, K.W.: Eocene bio-geochronology of ODP Leg 122 Hole 762C, Exmouth Plateau (northwest Australian Shelf), Stratigraphy, 9, 55-76, 2012.

Sims, P.A., Mann, D.G., Medlin, L.K.: Evolution of the diatoms: insights from fossil, biological and molecular data, Phycologia, 45, 361-402, 2006.

Sinton, C. W., Duncan R. A.: 40Ar/39Ar ages of lavas from the southeast Greenland margin, ODP Leg 152, and the Rockall Plateau, DSDP Leg 81, in: Sc. Res. Oc. Drill. Progr. 152, College Station, TX, Larsen, H.C., Saunders, A.P., Clift, P.D., 387– 402, 1998.

Slotnik, B.S., Dickens, G.R., Nicolo, M.J., Hollis, C.J., Crampton, J.S., Zachos, J.C., Sluijs, A.: Large-amplitude variations in carbon cycling and terrestrial weathering during the latest Paleocene and earliest Eocene: The Record at Mead Stream, New Zealand, J. Geol., 120, 487–505, 2012.

931

932 Smith, R.Y., Greenwood, D.R., Basinger, J. F.: Estimating paleoatmospheric pCO_2 during the Early
933 Eocene Climatic Optimum from stomatal frequency of Ginkgo, Okanagan Highlands, British
934 Columbia, Canada, Palaeogeogr. Palaeoclimatol. Palaeoecol., 293, 120–131, 2010.
935
936 Stanley, S.M.: Influence of seawater chemistry on biomineralization throughout Phanerozoic time:
937 paleontological and experimental evidence, Palaeogeogr. Palaeoclimatol. Palaeoecol., 232, 214–236.
938 doi: 10.1016/j.palaeo.2005.12.010, 2006.
939
940 Stanley, S.M.: Effect of Global Seawater Chemistry on Biomineralization: Past, Present, and Future,
941 Chem. Rew., 108, 4483-4498. Doi: 10.1021/cr800233u, 2008.
942
943 Stanley, S.M., Ries, J.B., Hardie, L.A.: Seawater chemistry, coccolithophore population growth, and
944 the origin of Cretaceous chalk, Geology 33, 593–596, 2005.
945
946 Thomas, E.: Biogeography of the late Paleocene benthic foraminiferal extinction, in Aubry, M.-P., et
947 al. (eds.), Late Paleocene–Early Eocene Climatic and Biotic Events in the Marine and Terrestrial
948 records: Columbia University Press, New York, p. 214–243, 1998.
949
950 Vandenberghe N., Hilgen F.J., Speijer R.P., Ogg J.G., Gradstein F.M., Hammer 0., Hollis C.J., Hooker
951 J.J., In: The Paleogene Period, In: Gradstein, F., Ogg, J.G., Schmitz, M.D., Ogg, G.M., The Geologic
952 Time Scale 2012, 855-921, Elsevier, Amsterdam, 2012.
953
954 Vogt, P.R.: Global magmatic episodes: New evidence and implications for the steady state mid-oceanic
955 ridge, Geology, 7, 93–98, 1979.
956
957 Wade, B. S.: Planktonic foraminiferal biostratigraphy and mechanisms in the extinction of *Morozovella*
958 in the late Middle Eocene, Mar. Micropaleont., 51, 23–38, 2004.
959

960 Wade, B.S., Al-Sabouni, N., Hemleben, C., Kroon, D.: Symbiont bleaching in fossil planktonic
961 foraminifera, Evol. Ecol., 22, 253-265. doi:10.1007/s10682-007-9176-6, 2008.
962
963 Wade, B.S., Pearson, P.N., Berggren, W.A., Pälike, H.: Review and revision of Cenozoic tropical
964 planktonic foraminiferal biostratigraphy and calibration to the geomagnetic polarity and astronomical
965 time scale, Earth Sci. Rev., 104, pp.111-142. doi:10.1016/j.earscirev.2010.09.003, 2011.
966
967 Wade, B.S., Fucek, V.P., Kamikuri, S.-I., Bartol, M., Luciani, V., Pearson, P.N.: Successive extinctions
968 of muricate planktonic foraminifera (*Morozovelloides* and *Acarinina*) as a candidate for marking the
969 base Priabonian. Newsletters on Stratigraphy, 45 (3) 245-262, 2012.
970
971 Westerhold, T., Röhl, U.: Orbital pacing of Eocene climate during the Middle Eocene Climate
972 Optimum and the chron C19r event–missing link found in the tropical western Atlantic, Geochem.,
973 Geophys., Geosyst., 14, 4811-4825, doi:10.1002/2013GC004960, 2013.
974
975 Wilf, P., Cúneo, R.N., Johnson, K.R., Hicks, J.F., Wing, S.L., Obradovich, J.D.: High plant diversity in
976 Eocene South America: evidence from Patagonia, Science, 300, 122-125, 2003.
977
978 Wing, S.L., Bown, T.M., Obradovich, J.D.: Early Eocene biotic and climatic change in interior western
979 North America, Geology 19, 1189-1192, 1991.
980
981 Woodbourne, M.O., Gunnell, G.F., Stucky, R.K.: Climate directly influences Eocene mammal faunal
982 dynamics in North America, PNAS, 106, 13399-13403, 2009.
983
984 Zachos, J.C., Pagani, M., Sloan, L., Thomas, E., Billups, K.: Trends, rhythms, and aberrations in global
985 climate 65 Ma to Present, Science, 292, 686–693, 2001.
986
987 Zachos, J.C., Röhl, U., Schellenberg, S.A., Sluijs, A., Hodell, D.A., Kelly, D.C., Thomas, E., Nicolo,
988 M., Raffi, I., Lourens, L.J., McCarren, H., Kroon, D.: Rapid acidification of the ocean during the
989 Paleocene–Eocene thermal maximum, Science, 308, 1611–161, 2005.

Zachos, J.C., S. Schouten, S. Bohaty, T., Quattlebaum, Sluijs, A., Brinkhuis, H., Gibbs, S.J., Bralower, T.J.: Extreme warming of midlatitude coastal ocean during the Paleocene-Eocene thermal maximum: Inferences from TEX86 and isotope data, Geology, 34(9), 737–740. doi:10.1130/G22522.1, 2006.

Zachos, J.C., Dickens, G. R., Zeebe, R.E.: An early Cenozoic perspective on greenhouse warming and carbon-cycle dynamics, Nature, 451, 279–283, 2008.

Zachos, J.C., McCarren, H., Murphy, B., Röhl, U., Westerhold, T.: Tempo and scale of late Paleocene and early Eocene carbon isotope cycles: Implications for the origin of hyperthermals, Earth Planet. Sci. Lett., 299, 242-249, doi:10.1016/j.epsl.2010.09.004, 2010.

Zeebe, R.E., Zachos, J.C., Caldeira K., Tyrrel T.: Carbon emissions and acidification, Science, 321, 51-52, 2008.

Zonneveld, J.P., Gunnell, G.F., Bartels, W.S.: Early Eocene fossil vertebrates from the southwestern Green River Basin, Lincoln and Uinta Counties, Wyoming, J. Vert. Paleontol., 20, 369-386, 2000.

Figure Captions

Figure 1. Left: Paleogeographic location of the Possagno section (star) in the Belluno Basin, a Mesozoic–Cenozoic pelagic sequence, delimited during the Eocene by the shallow water carbonates of the Lessini Shelf to the west (Modified from Bosellini, 1989). 1 - deep water mudstones of the Jurassic basins; 2 - Paleogene shallow water limestones, lagoons, and shelf-edge reefs of the Lessini Shelf; 3 - Paleogene deep water pelagic claystones and marlstones of the Belluno and Lombardian Basin. Right: Blake Nose map and location of Site 1051 in the western North Atlantic, modified from Norris et al. (1998).

Figure 2. Carbon and oxygen isotopes of bulk sediment from the Possagno section plotted against lithology and planktic foraminiferal E-Zonations from Wade et al. (2011), modified by Luciani and Giusberti (2014). Magnetostratigraphy is from Agnini et al. (2006). Thinner lines: original data; thicker lines average 3-points. The average 3-point curve is utilized to dampen some of the potential diagenetic overprint on the ^{18}O data. The red line is referred to the stable carbon isotopes and the blue line to the oxygen data. Pre-EECO CIEs are labelled according to current literature; the EECO and post-EECO CIEs are labelled according to Kirtland Turner et al. (2014) and Sexton et al. (2011) by substituting H (hyperthermals) with CIE (carbon isotope excursion). The yellow band band highlights the interval tentatively referred to the EECO. We have tentatively named the post-EECO isotope shifts of small magnitude as events only when changes in isotopic composition are associated with sharp variations in planktic foraminferal assemblages and/or fragmentation index. This is because increase in fragmentation index as well as increase in some taxa have been observed during the pre-EECO hyperthermals from the same geological setting (Luciani et al. 2007; Agnini et al., 2009). However, since the identification of some post-EECO minor shifts as hyperthermals is tentative, they are indicated with a question mark. Filled circles show occurrences of abundant radiolarians.

Fig. 3. The Possagno $\delta^{13}C$ record and relative abundance of main planktic foraminifera across the early and basal middle Eocene interval, plotted against lithology, fragmentation index (*F* index) and coarse fraction (CF) data. The subbotinids includes the genera *Subbotina* and *Parasubbotina*. Magnetostratigraphy is from Agnini et al. (2006). The biozonal scheme is from Wade et al. (2011), modified by Luciani and Giusberti (2014). The yellow bands highlight the interval tentatively referred to the EECO, the pre-EECO hyperthermals and post-EECO stable isotope excursions that are considered to represent hyperthermals. Pre-EECO CIEs are labelled according to current literature; the EECO and post-EECO CIEs are labelled according to Kirtland Turner et al. (2014) and Sexton et al. (2011) by substituting H (hyperthermals) with CIE (carbon isotope excursion). We have tentatively named the post-EECO isotope shifts of small magnitude as events only when changes in isotopic composition are associated with sharp variations in planktic foraminferal assemblages and/or fragmentation index. This is because increase in fragmentation index as well as increase in acarininid abundance have been observed during the pre-EECO hyperthermals from the same geological setting

(Luciani et al. 2007; Agnini et al., 2009). However, since the identification of some post-EECO minor shifts as hyperthermals is tentative, they are indicated with a question mark. Filled circles show occurrences of abundant radiolarians.

Fig. 4. Relative abundance of the main planktic foraminiferal genera from ODP Site 1051, plotted against the biozones of Wade et al. (2011), partly modified by Luciani and Giusberti (2014), and *F* index data. The subbotinid group includes the genera *Subbotina* and *Parasubbotina*. Magnetostratigraphy is from Ogg and Bardot (2001); the gray bands are intervals of uncertainty in magnetostratigraphic boundaries. The striped band is an interval of non-recovery. The yellow band highlights the interval tentatively referred to the EECO.

Figure 5. The record of warm-indices muricates morozovellids and large acarininids (>200 micron) in the western Tethyan setting from the Possagno (below, this paper) and Alano sections (above, from Luciani et al., 2010) plotted against the generalized oxygen and carbon isotopic curves based on benthic foraminiferal record, slightly modified, shown in Vandenberghe et al. (2012, Fig. 28.11). The original oxygen and carbon isotopic values from Cramer et al. (2009) are recalibrated to GTS2012 (Vandenberghe et al., 2012). The Tethyan record shows that the long-lasting EECO and MECO intervals mark two main steps in the decline of relative abundance within this group of important early Paleogene calcifiers. E-Zones follow Wade et al. (2011), partly modified by Luciani and Giusberti (2014). B-P=Bartonian-Priabonian.

Table 1. Position with respect to magnetochrons of nine early and lower-middle Eocene $\delta^{13}C$ shifts (CIE) at the Possagno section. The analogous magnetostratigraphic position of the hyperthermals (H) recognized at Site 1258, Demerara Rise (Kirtland Turner et al, 2014; Sexton et al., 2011) suggests a possible correspondence of these events.

Appendix A. Supplementary material

Table S1. Possagno $\delta^{13}C$ (‰) and $\delta^{18}O$ (‰) values against thickness (meters).

Figure S1. The Possagno $\delta^{13}C$ data and relative abundance of minor planktic foraminiferal genera and selected species plotted against lithology, fragmentation index (*F* index) data. Magnetostratigraphy is from Agnini et al. (2006). The biozonal scheme is from Wade et al. (2011), modified by Luciani and Giusberti (2014). The yellow bands highlight the interval tentatively referred to the EECO, the pre-EECO hyperthermals and post-EECO stable isotope excursions that are considered to represent hyperthermals. Pre-EECO CIEs are labelled according to current literature; the EECO and post-EECO CIEs are labelled according to Sexton et al. (2011) by substituting H (hyperthermals) with CIE (carbon isotope excursion). We have tentatively named the post-EECO isotope shifts of small magnitude as events only when changes in isotopic composition are associated with sharp variations in planktic foraminferal assemblages and/or fragmentation index. This is because increase in fragmentation index as well as increase in acarininid abundance have been observed during the pre-EECO hyperthermals from the same geological setting (Luciani et al. 2007; Agnini et al., 2009). However, since the identification of some post-EECO minor shifts as hyperthermals is tentative, they are indicated with a question mark. Filled circles show occurrences of abundant radiolarians.

Appendix B. Taxonomic list of species cited in text and figures

Globanomalina australiformis (Jenkins, 1965)

Morozovella aequa (Cushman and Renz, 1942)

Morozovella gracilis (Bolli, 1957)

Morozovella lensiformis (Subbotina, 1953),

Morozovella marginodentata (Subbotina, 1953)

Morozovella subbotinae (Morozova, 1939)

Parasubbotina eoclava Coxall, Huber and Pearson, 2003

Parasubbotina griffinae (Blow, 1979)

Parasubbotina pseudowilsoni Olsson and Pearson, 2006

Subbotina corpulenta (Subbotina, 1953)

Subbotina eocena (Guembel, 1868)

Subbotina hagni (Gohrbandt, 1967)

Subbotina senni (Beckmann, 1953)

Subbotina yeguanesis (Weinzierl and Applin, 1929*)*

Planoglobanomalina pseudoalgeriana Olsson & Hemleben, 2006

Fig. 1

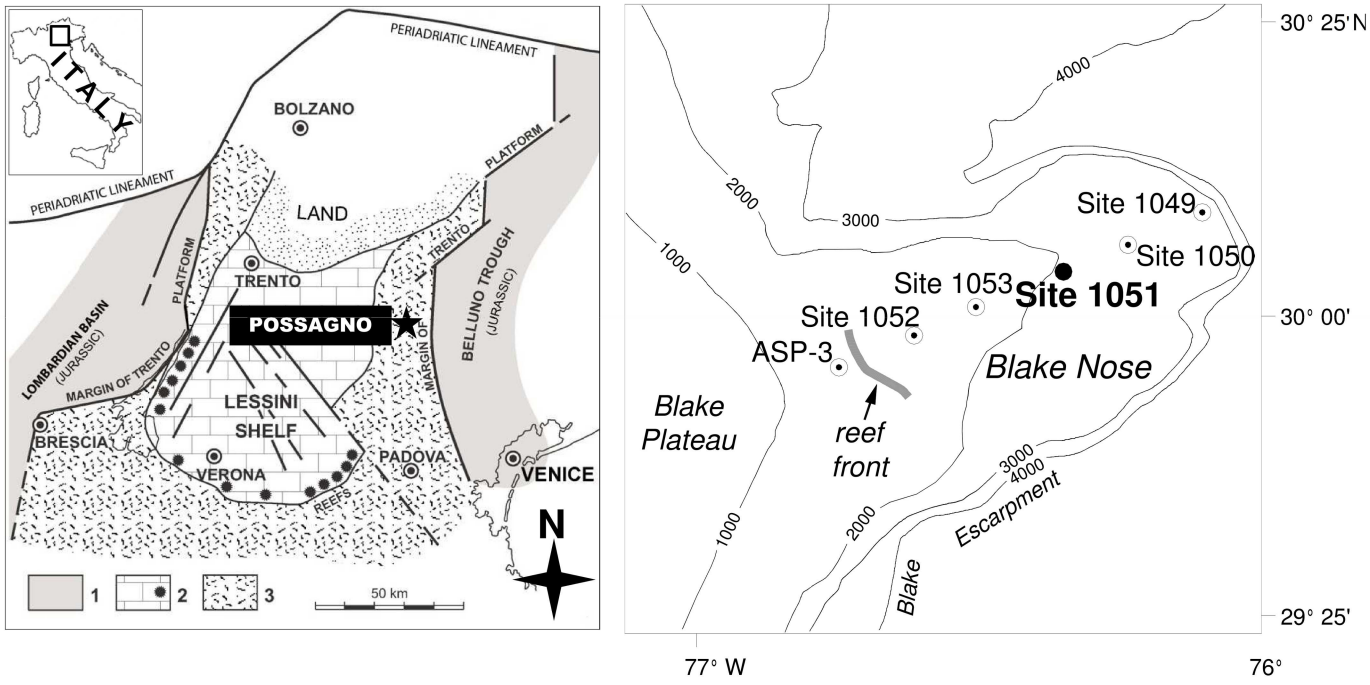
ITALY
PERIADRIATIC LINEAMENT
BOLZANO
PERIADRIATIC LINEAMENT
PLATFORM
LAND
TRENTO
PLATFORM
TRENTO
BELLUNO TROUGH
(JURASSIC)
LOMBARDIAN BASIN
(JURASSIC)
MARGIN OF TRENTO
POSSAGNO
MARGIN OF
LESSINI
SHELF
BRESCIA
VERONA
REEFS
PADOVA
VENICE
N
1
2
3
50 km
4000
2000
3000
1000
Site 1049
Site 1050
Site 1053
Site 1051
Site 1052
ASP-3
Blake Nose
Blake
Plateau
reef
front
3000
4000
Escarpment
2000
1000
Blake
30° 25'N
30° 00'
29° 25'
77° W
76°

Fig. 2

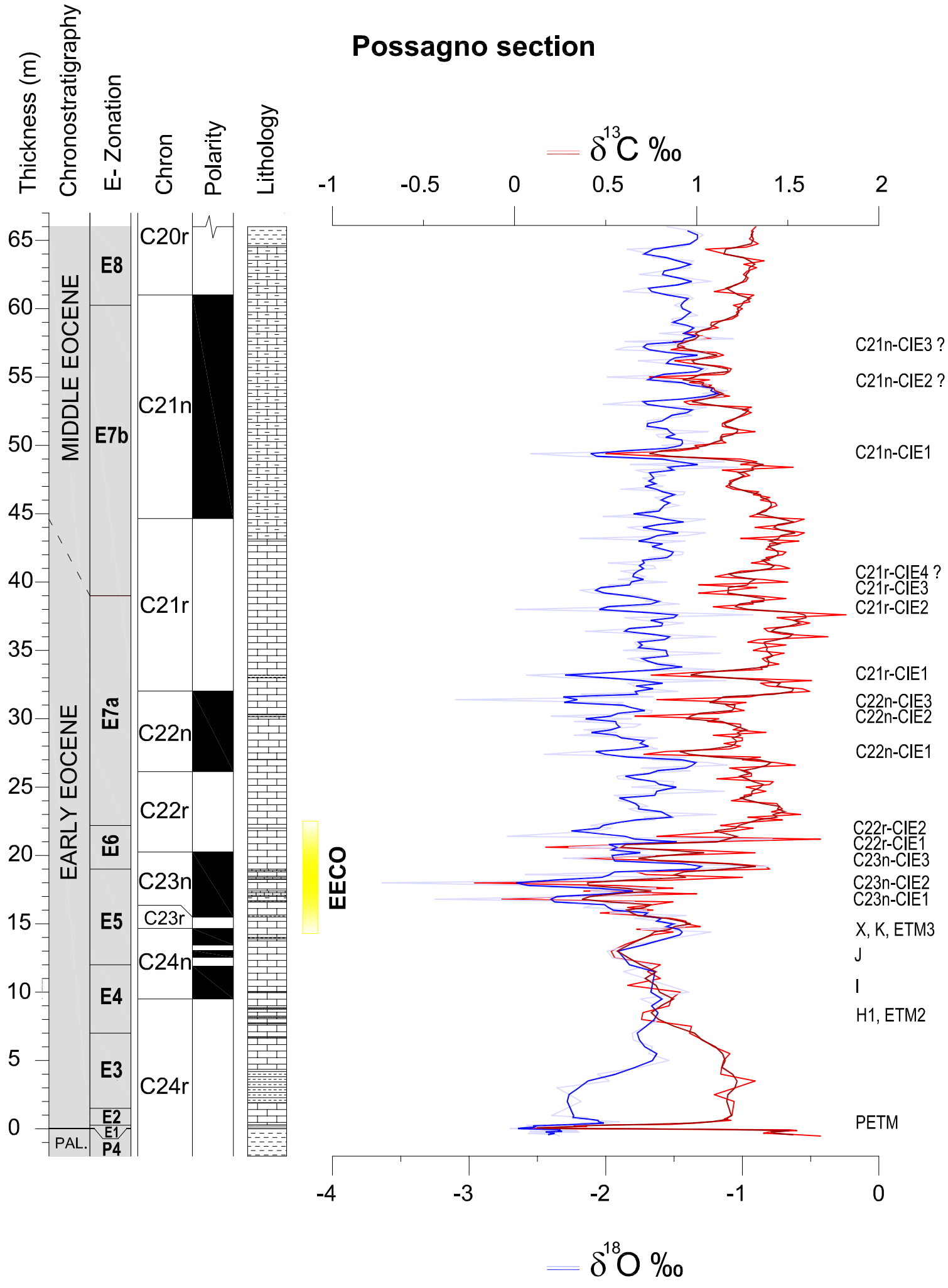
Possagno section
Thickness (m)
Chronostratigraphy
E- Zonation
Chron
Polarity
Lithology
MIDDLE EOCENE
EARLY EOCENE
E8
E7b
E7a
E6
E5
E4
E3
E2
E1
P4
PAL.
C20r
C21n
C21r
C22n
C22r
C23n
C23r
C24n
C24r
65
60
55
50
45
40
35
30
25
20
15
10
5
0
δ13C ‰
-1
-0.5
0
0.5
1
1.5
2
EECO
C21n-CIE3 ?
C21n-CIE2 ?
C21n-CIE1
C21r-CIE4 ?
C21r-CIE3
C21r-CIE2
C21r-CIE1
C22n-CIE3
C22n-CIE2
C22n-CIE1
C22r-CIE2
C22r-CIE1
C23n-CIE3
C23n-CIE2
C23n-CIE1
X, K, ETM3
J
I
H1, ETM2
PETM
-4
-3
-2
-1
0
δ18O ‰

Fig. 3

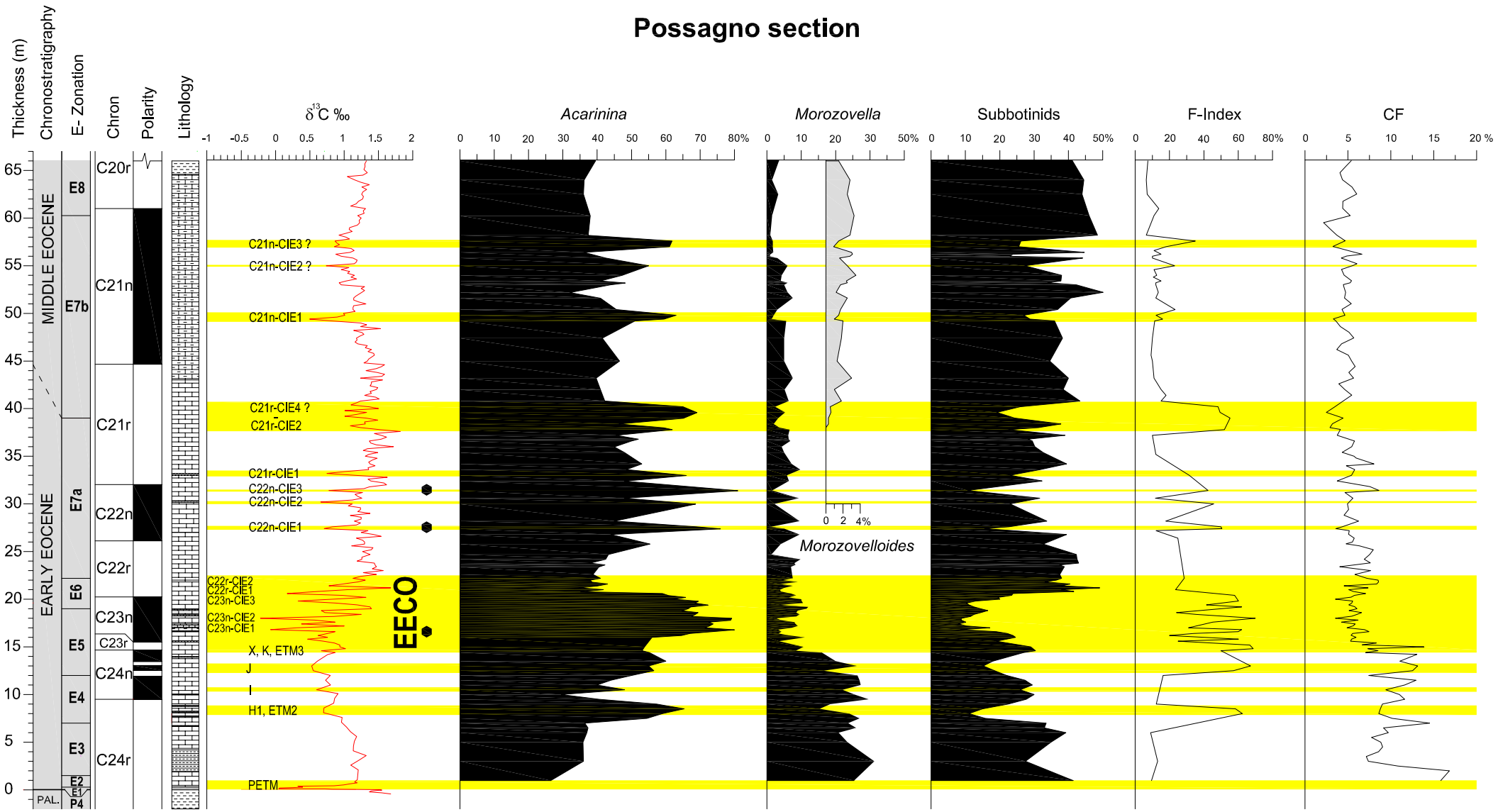
Possagno section
Thickness (m)
Chronostratigraphy
E- Zonation
Chron
Polarity
Lithology
δ13C ‰
Acarinina
Morozovella
Morozovelloides
Subbotinids
F-Index
CF
MIDDLE EOCENE
EARLY EOCENE
E8
E7b
E7a
E6
E5
E4
E3
E2
E1
P4
PAL.
C20r
C21n
C21r
C22n
C22r
C23n
C23r
C24n
C24r
C21n-CIE3 ?
C21n-CIE2 ?
C21n-CIE1
C21r-CIE4 ?
C21r-CIE2
C21r-CIE1
C22n-CIE3
C22n-CIE2
C22n-CIE1
C22r-CIE2
C22r-CIE1
C23n-CIE3
C23n-CIE2
C23n-CIE1
X, K, ETM3
J
I
H1, ETM2
PETM
EECO

Fig. 4

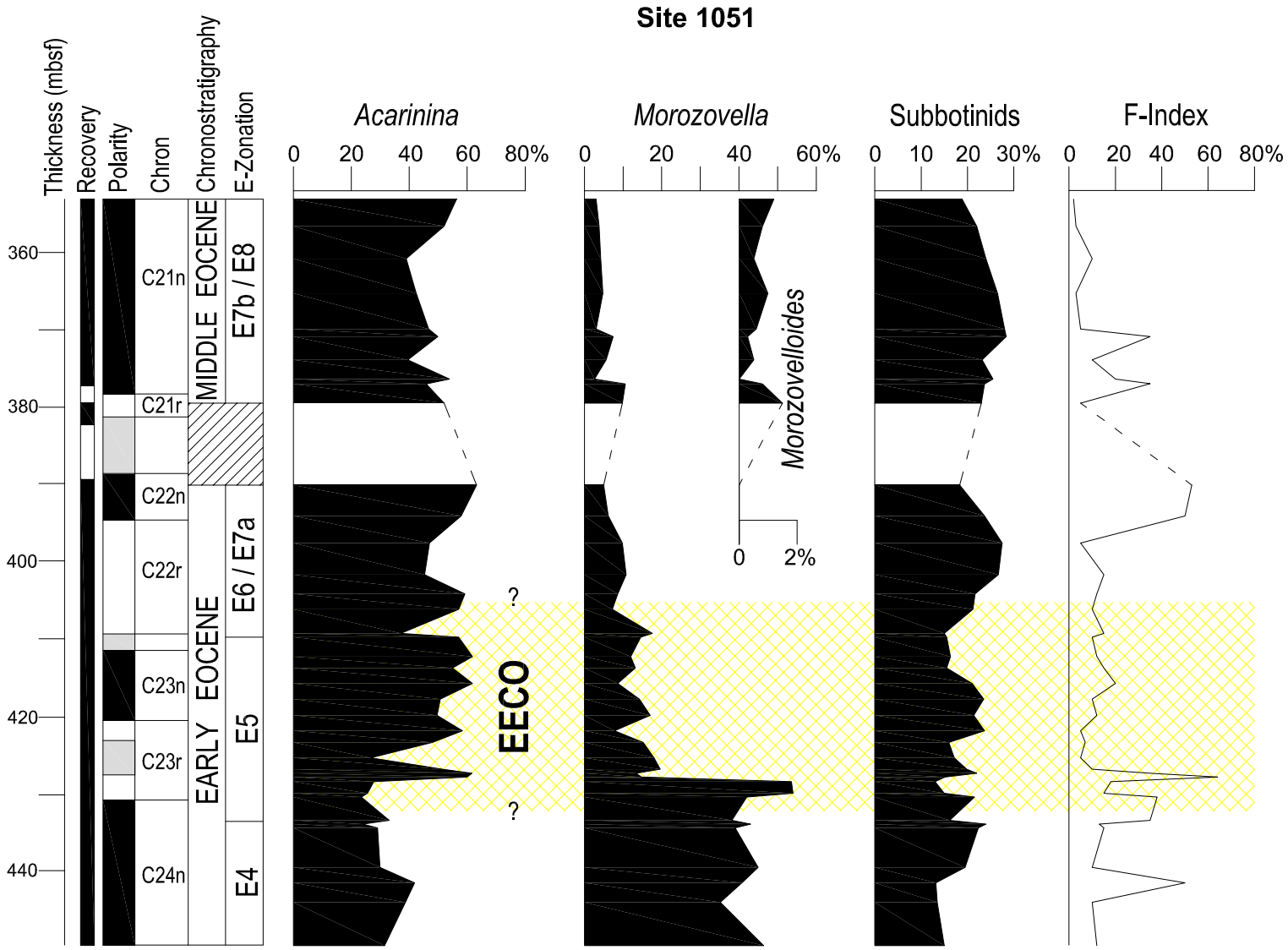
Site 1051
Thickness (mbsf)
Recovery
Polarity
Chron
Chronostratigraphy
E-Zonation
360
380
400
420
440
C21n
C21r
C22n
C22r
C23n
C23r
C24n
MIDDLE EOCENE
EARLY EOCENE
E7b / E8
E6 / E7a
E5
E4
Acarinina
0 20 40 60 80%
Morozovella
0 20 40 60%
Morozovelloides
0 2%
Subbotinids
0 10 20 30%
F-Index
0 20 40 60 80%
EECO
?
?

Fig. 5

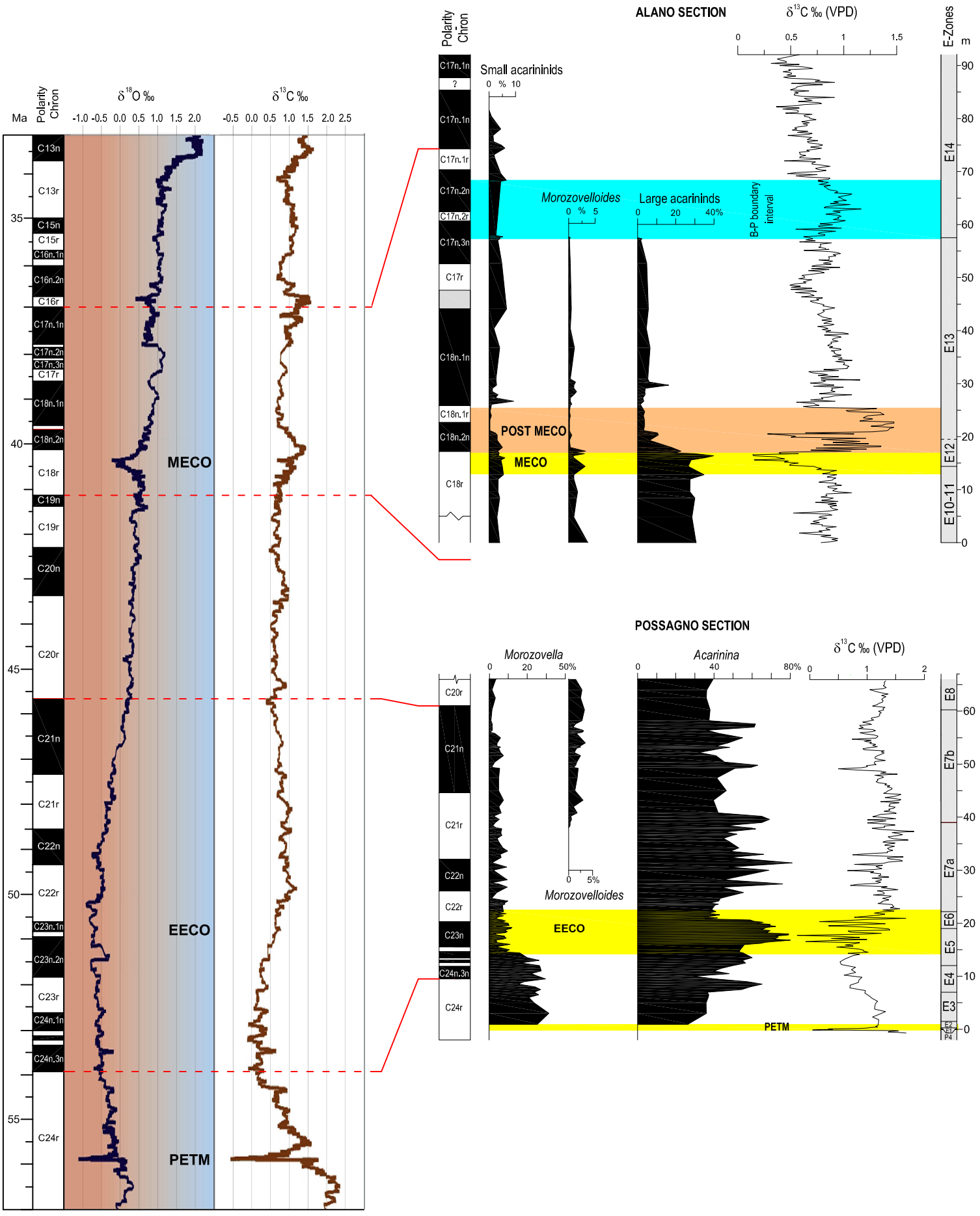
Ma
Polarity Chron
δ18O ‰
δ13C ‰
-1.0 -0.5 0.0 0.5 1.0 1.5 2.0
-0.5 0.0 0.5 1.0 1.5 2.0 2.5
C13n
C13r
C15n
C15r
C16n.1n
C16n.2n
C16r
C17n.1n
C17n.2n
C17n.3n
C17r
C18n.1n
C18n.2n
C18r
C19n
C19r
C20n
C20r
C21n
C21r
C22n
C22r
C23n.1n
C23n.2n
C23r
C24n.1n
C24n.3n
C24r
35
40
45
50
55
MECO
EECO
PETM
ALANO SECTION
δ13C ‰ (VPD)
E-Zones
m
Small acarininids
0 % 10
Morozovelloides
0 % 5
Large acarininds
0 20 40%
B-P boundary interval
POST MECO
MECO
E14
E13
E12
E10-11
POSSAGNO SECTION
Morozovella
0 20 50%
Acarinina
0 40 80%
0 1 2
0 5%
Morozovelloides
EECO
PETM
E8
E7b
E7a
E6
E5
E4
E3
P4

Table 1.

MAGNETOCHRON	POSSAGNO (NORTHEASTERN ITALY)	*DEMERARA RISE (ODP SITE 1258, WESTERN TROPICAL ATLANTIC)*
	STABLE CARBON ISOTOPE SHIFTS	***HYPERTHERMAL EVENTS***
C21r	CIE4	*H4*
	CIE3	*H3*
	CIE2	*H2*
	CIE1	*H1*
C22n	CIE3	*H3*
	CIE2	*HE*
	CIE1	*H1*
C22r	CIE2	*H2*
	CIE1	*H1*

Supplementary material

Fig. S1

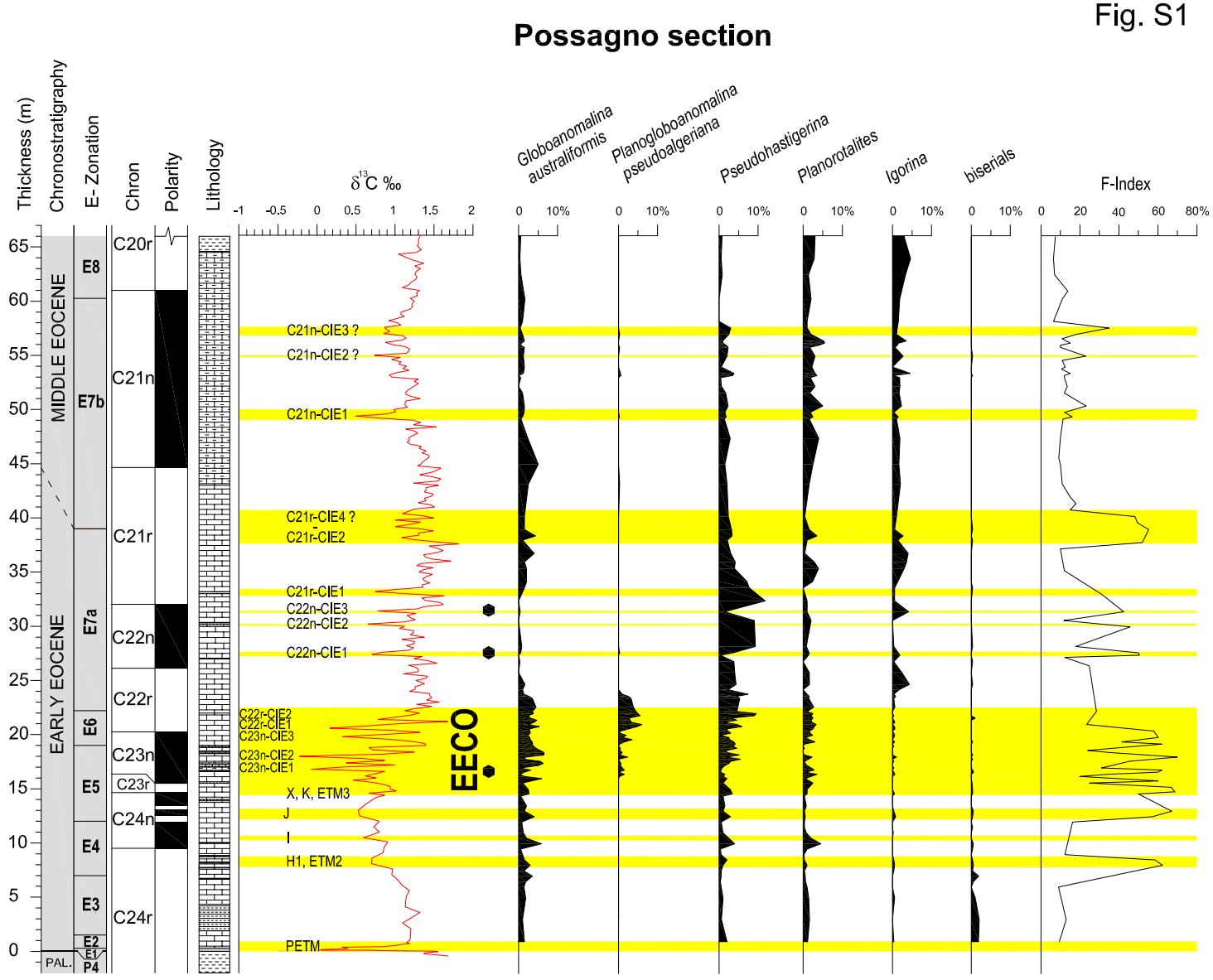
Possagno section
Thickness (m)
Chronostratigraphy
E- Zonation
Chron
Polarity
Lithology
δ13C ‰
Globoanomalina australiformis
Planoglobanomalina pseudoalgeriana
Pseudohastigerina
Planorotalites
Igorina
biserials
F-Index
MIDDLE EOCENE
EARLY EOCENE
E8
E7b
E7a
E6
E5
E4
E3
E2
E1
P4
PAL.
C20r
C21n
C21r
C22n
C22r
C23n
C23r
C24n
C24r
C21n-CIE3 ?
C21n-CIE2 ?
C21n-CIE1
C21r-CIE4 ?
C21r-CIE2
C21r-CIE1
C22n-CIE3
C22n-CIE2
C22n-CIE1
C22r-CIE2
C22r-CIE1
C23n-CIE3
C23n-CIE2
C23n-CIE1
EECO
X, K, ETM3
J
I
H1, ETM2
PETM

Table S1. Isotopic data of Possagno section

Thickness (meters)	d13Cpdb ‰	d18Opdb ‰
66	1,324503865	-1,554131513
65,7	1,301202621	-1,363687878
65,4	1,306330409	-1,285765533
65,1	1,289525476	-1,334902053
65,1	1,288019147	-1,361227875
64,75	1,337699738	-1,365512853
64,5	1,271493282	-1,449946289
64,35	1,048026588	-1,843804126
64	1,157592263	-1,664853101
63,75	1,242287722	-1,654166107
63,5	1,369396415	-1,354916697
63,25	1,258468714	-1,405387406
63	1,328439322	-1,377815013
62,75	1,277403321	-1,585307364
62,5	1,255599346	-1,755604391
62,25	1,28272387	-1,411073928
62	1,268756475	-1,226212864
61,75	1,209940758	-1,47335947
61,5	1,178018179	-1,715059881
61,25	1,095738735	-1,870218997
61	1,313557115	-1,399695163
60,75	1,277940478	-1,35860539
60,5	1,291423645	-1,430644636
60,25	1,200942841	-1,498587494
60	1,250952568	-1,417450314
59,75	1,218475547	-1,393167024
59,5	1,225717988	-1,324035769
59,25	1,194266763	-1,51954699
59	1,080495861	-1,482955818
58,8	1,075773802	-1,522460465
58,6	1,11857554	-1,22201932
58,4	1,028116908	-1,323055034
58,2	0,92447057	-1,608414416
58	1,028708603	-1,348841195
57,8	1,07809129	-1,064679508
57,6	0,87	-1,86
57,4	0,892621305	-1,393869643
57,2	0,932505455	-1,848349814
57	0,858608928	-1,928927784
56,8	1,10415658	-1,260469084
56,6	1,146353927	-1,451587324
56,4	1,086170402	-1,271435385
56,2	0,878456082	-1,761198406
56	0,958974626	-1,566232448
55,8	1,131602612	-1,334447985
55,6	1,19	-1,25
55,4	1,18	-1,29

55,2	1,15	-1,45
55	0,74	-1,99
54,8	1,07	-1,5
54,6	0,96	-1,58
54,4	1,08	-1,25
54,2	1,05	-1,29
54	1,15	-1,11
53,8	1,1	-1,29
53,6	1,18	-1,14
53,4	1,03	-1,36
53,2	0,93	-1,8
53	0,96	-2,02
52,8	1,3	-1,26
52,6	1,25	-1,36
52,4	1,3	-1,48
52,2	1,26	-1,37
51,8	1,17	-1,7
51,6	1,14	-1,69
51,4	1,14	-1,69
51,2	1,21	-1,71
51	1,32	-1,25
50,8	1,14	-1,63
50,6	1,13	-1,61
50,4	1,13	-1,44
50,2	1,16	-1,28
50	0,99	-1,59
49,8	1,01	-1,48
49,6	0,9	-1,57
49,4	0,5	-2,55
49,2	0,82	-2,21
49	1,24	-1,43
48,8	1,33	-1,13
48,6	1,24	-1,82
48,4	1,53	-1,03
48,2	1,14	-1,78
48	1,26	-1,7
47,8	1,29	-1,56
47,6	1,23	-1,73
47,4	1,18	-1,65
47,2	1,19	-1,67
47	1,16	-1,58
46,8	1,2	-1,89
46,6	1,34	-1,42
46,4	1,31	-1,43
46,2	1,4	-1,64
46	1,35	-1,59
45,8	1,43	-1,55
45,6	1,44	-1,46
45,2	1,36	-1,71
45	1,34	-1,66

44,8	1,29	-2,02
44,6	1,59	-1,27
44,4	1,54	-1,41
44,2	1,47	-1,61
44	1,32	-1,84
43,8	1,48	-1,73
43,6	1,59	-1,27
43,4	1,55	-1,41
43,2	1,24	-2,19
43	1,56	-1,42
42,8	1,4	-1,67
42,6	1,4	-1,66
42,4	1,38	-1,65
42,2	1,49	-1,43
42	1,47	-1,44
41,8	1,38	-1,69
41,6	1,4	-1,52
41,4	1,3	-1,98
41,2	1,46	-1,65
41	1,51	-1,63
40,8	1,24	-1,89
40,6	1,18	-1,78
40,4	1,1	-1,71
40,2	1,36	-1,91
40	1,5	-1,55
39,8	1,01	-1,98
39,6	1,33	-1,94
39,4	1,18	-2,19
39,2	1,01	-2,09
39	1,32	-1,75
38,8	1,49	-1,66
38,6	1,3	-1,71
38,4	1,31	-1,46
38,2	1,09	-1,83
38	1,24	-2,66
37,8	1,52	-1,65
37,6	1,82	-0,92
37,4	1,44	-1,86
37,2	1,54	-1,72
37	1,62	-1,43
36,8	1,54	-1,6
36,6	1,37	-1,74
36,4	1,39	-2,15
36,2	1,47	-1,69
36	1,72	-1,19
35,8	1,34	-1,72
35,6	1,28	-1,79
35,4	1,49	-1,77
35,2	1,36	-1,64
35	1,31	-1,87

34,8	1,48	-1,16
34,6	1,41	-1,63
34,4	1,36	-1,84
34,2	1,38	-1,73
34	1,45	-1,49
33,8	1,35	-1,63
33,6	1,36	-1,2
33,4	1	-2,02
33,2	0,75	-2,58
33	1,15	-2,29
32,8	1,63	-1,12
32,6	1,35	-1,84
32,4	1,39	-1,79
32,2	1,58	-1,7
32	1,62	-1,47
31,8	1,37	-2,18
31,6	1,29	-1,65
31,4	0,78	-3,1
31,2	1,27	-1,87
31	1,16	-1,94
30,8	1,2	-1,81
30,6	1,26	-1,66
30,4	1,12	-1,67
30,2	0,66	-2,4
30	1,12	-1,81
29,8	1,06	-2,23
29,6	1,24	-1,74
29,4	1,24	-1,79
29,2	1,2	-2,16
29	1,38	-1,92
28,8	1,09	-2,23
28,6	1,25	-1,62
28,4	1,25	-1,8
28,2	1,15	-1,74
28	1,24	-1,7
27,8	1,18	-1,62
27,6	0,83	-2,15
27,4	0,71	-2,45
27,2	1,35	-1,41
27	1,25	-1,66
26,8	1,43	-1,25
26,6	1,54	-1,11
26,4	1,18	-1,74
26,2	1,27	-1,38
26	1,3	-1,74
25,8	1,3	-1,92
25,6	1,11	-1,91
25,4	1,42	-1,5
25,2	1,4	-1,51
25	1,27	-1,81

24,7	1,38	-1,13
24,4	1,26	-1,94
24,2	1,26	-1,85
24	1,19	-1,91
23,8	1,44	-1,75
23,6	1,45	-1,69
23,4	1,47	-1,83
23,2	1,41	-1,76
23	1,57	-1,19
22,8	1,28	-1,72
22,6	1,47	-1,64
22,4	1,25	-1,99
22,2	1,13	-2,11
22	1,31	-1,96
21,8	1,2	-2,07
21,4	0,78	-2,72
21,2	1,68	-0,78
21	1,05	-1,87
20,8	0,61	-1,79
20,6	0,17	-2,27
20,4	0,97	-1,69
20,2	1,32	-1,91
20	0,83	-1,64
19,8	0,33	-2,31
19,6	0,88	-1,89
19,4	1,19	-1,6
19,2	1,38	-0,81
19	1,4	-1,49
18,8	0,67	-1,73
18,6	0,72	-2,59
18,4	1,25	-1,59
18,2	0,85	-1,9
18	-0,22	-3,64
17,8	0,57	-2,43
17,6	0,87	-1,63
17,4	0,38	-2,11
17,2	1	-1,66
17	0,31	-2,16
16,8	-0,07	-3,25
16,6	0,87	-1,79
16,4	0,76	-2,08
16,2	0,62	-2,16
16	0,76	-1,7
15,8	0,47	-1,97
15,6	0,7	-1,41
15,4	0,86	-1,79
15,2	0,94	-1,58
15	0,94	-1,51
14,8	1,02	-1,42
14,6	0,67	-1,74

14,4	0,87	-1,23
14,2	0,76	-1,35
13,5	0,61	-1,79
13	0,53	-1,99
12,55	0,55	-1,95
12	0,8	-1,66
11,5	0,73	-1,87
10	0,91	-1,39
9,5	0,860407617	-1,745868284
9	0,847698043	-1,6249864
8,5	0,704323168	-1,620825392
8	0,697123094	-1,606233422
7,5	0,971220119	-1,70465462
7	0,960200544	-1,804953966
6,5	1,03282727	-1,798588563
6	1,093247595	-1,655217488
5,5	1,182569921	-1,685192373
5	1,147446246	-1,536443685
4,5	1,136631571	-1,751460814
4	1,131549897	-2,060952576
3,5	1,321208222	-1,972329429
3	1,210211548	-2,357527232
2,5	1,095834873	-2,265978774
2	1,205609198	-2,180916572
0,975	1,193025524	-2,39513048
0,825	1,169705849	-2,128674243
0,725	1,150951175	-2,193656665
0,625	1,187252381	-2,071204006
0,525	1,072769571	-1,900119279
0,425	0,996418462	-2,185873828
0,325	0,855189052	-1,957644402
0,275	0,325183243	-2,571328228
0,225	0,363733114	-2,577693458
0,175	0,395223833	-2,442193443
0,125	0,261679624	-2,517606276
0,075	0,056425765	-2,600329725
0,025	0,046204045	-2,697877737
0,01	0,715394386	-2,627456411
-0,025	0,825253976	-2,496448436
-0,075	1,512990667	-2,286158599
-0,125	1,549820857	-2,208348633
-0,175	1,458455048	-2,554977403
-0,225	1,393471238	-2,195702997
-0,325	1,366631429	-2,565834405
-0,425	1,545594619	-2,359719334
-0,525	1,67926181	-2,339723417
-0,725	1,762957082	-2,045519714
-0,825	1,772335157	-1,765052919